Molecular Plant Advance Access published February 17, 2014

Role of *Arabidopsis UV RESISTANCE LOCUS 8* in Plant Growth Reduction under Osmotic Stress and Low Levels of UV-B

Rossella Fasano[a], Nathalie Gonzalez[b,c], Alessandra Tosco[a], Fabrizio Dal Piaz[a], Teresa Docimo[d], Ramon Serrano[e], Stefania Grillo[f], Antonella Leone[a], and **Dirk Inzé[b,c,1]**

a Department of Pharmacy, University of Salerno, Fisciano, Italy
b Department of Plant Systems Biology, VIB, 9052 Ghent, Belgium
c Department of Plant Biotechnology and Bioinformatics, Ghent University, 9052 Gent, Belgium
d Max Planck Institute for Chemical Ecology, Jena, Germany
e Instituto de Biología Molecular y Celular de Plantas, Universidad Politecnica de Valencia CSIC, Valencia, Spain
f National Research Council of Italy, Institute of Plant Genetics, Res. Div. Portici, Portici, Italy

ABSTRACT In high-light environments, plants are exposed to different types of stresses, such as an excess of UV-B, but also drought stress which triggers a common morphogenic adaptive response resulting in a general reduction of plant growth. Here, we report that the *Arabidopsis thaliana UV RESISTANCE LOCUS 8* (*UVR8*) gene, a known regulator of the UV-B morphogenic response, was able to complement a *Saccharomyces cerevisiae* osmo-sensitive mutant and its expression was induced after osmotic or salt stress in *Arabidopsis* plants. Under low levels of UV-B, plants overexpressing *UVR8* are dwarfed with a reduced root development and accumulate more flavonoids compared to control plants. The growth defects are mainly due to the inhibition of cell expansion. The growth inhibition triggered by *UVR8* overexpression in plants under low levels of UV-B was exacerbated by mannitol-induced osmotic stress, but it was not significantly affected by ionic stress. In contrast, *uvr8-6* mutant plants do not differ from wild-type plants under standard conditions, but they show an increased shoot growth under high-salt stress. Our data suggest that UVR8-mediated accumulation of flavonoid and possibly changes in auxin homeostasis are the underlying mechanism of the observed growth phenotypes and that UVR8 might have an important role for integrating plant growth and stress signals.

Key words: osmotic stress; growth reduction; cell expansion; flavonoid; auxin.

INTRODUCTION

Due to the sessile nature of plants, their growth can be affected by a combination of environmental stresses, such as drought, salinity, freezing, or excess UV light that greatly reduces yield in crop species. Amongst abiotic stresses, extreme temperatures, high salinity, and drought are the main environmental constraints to agricultural productivity worldwide (Cramer et al., 2011).

High salinity and water deficit are the major causes of osmotic stress in plants. The reaction of plants to water deficit differs significantly at various organizational levels depending on the stress intensity and duration, as well as on the developmental stage and the plant species (Chaves et al., 2002; Verslues et al., 2006). Plants have evolved different strategies to counteract osmotic stress. For example, they can close stomata to conserve water and accumulate osmolytes (e.g. proline, glycine-betaine, and oligosaccharides), restoring the osmotic potential of the cell by water uptake to maintain cell turgor (Xiong and Zhu, 2002). Plants also synthesize protective proteins, such as dehydrins, and antioxidant enzymes, such as catalases and superoxide dismutases, that protect proteins, membranes, and cellular components from accumulating reactive oxygen species (ROS), by reducing their levels.

An important physiological effect of mild drought on crops is the reduction in vegetative growth (Skirycz and Inzé, 2010) and in general shoot growth is more affected than root growth. Whereas, under water deficit, stem elongation and leaf growth of many important crops is greatly inhibited

[1] To whom correspondence should be addressed. E-mail dirk.inze@psb.ugent.be, tel. +32 (0)9 331 38 06, fax +32 (0)9 331 38 09.

doi:10.1093/mp/ssu002

Received 9 August 2013; accepted 4 January 2014

(Heuer and Nadler, 1995; Specht et al., 2001; Wu et al., 2008; Farooq et al., 2009), under mild osmotic stress, roots can continue to grow (Bartels and Sunkar, 2005; Pardo, 2010). Enhanced root growth also was observed in transgenic plants with a higher drought or salt-stress tolerance (Bartels and Sunkar, 2005; Werner et al., 2010). Furthermore, drought-tolerant rice (*Oryza sativa*) varieties have a deeper and more highly branched root system than drought-sensitive varieties (Price et al., 1997). The development of a larger root system is considered as a drought-avoidance strategy that plants adopt to improve the uptake of water and nutrients when their availability in the soil is limited (Fukai and Cooper, 1995; Liao et al., 2001; Sharp et al., 2004).

Similar differential impacts on shoot or root growth were also seen in plants grown under other abiotic stress conditions, such as exposure to heavy metals or phosphate starvation, that impact mainly roots, or excess UV-B radiation, that influences shoot growth. These architectural changes in plants facing different non-optimal external environmental conditions, which include a general reduction of plant size, are known as Stress Induced Morphogenic Response (SIMR; Potters et al., 2007, 2009). By reducing their growth, plants can conserve and redistribute resources and thus increase their chance of survival if the stress becomes severe. At a cellular level, in the leaf, plants respond to drought stress by a rapid initial growth reduction, followed by growth adaptation, leading to leaves with fewer and smaller cells (Claeys and Inzé, 2013).

Low-fluence (280–320 nm) UV-B light serves as an environmental stimulus to direct growth and development. This includes hypocotyl growth inhibition, reduction of leaf expansion or root growth, formation of shorter petioles, flavonoid accumulation, and specific gene expression (Kim et al., 1998; Boccalandro et al., 2001; Casimiro et al., 2001; Kliebenstein et al., 2002; Frohnmeyer and Staiger, 2003; Suesslin and Frohnmeyer, 2003; Ulm and Nagy, 2005; Hectors et al., 2010). The low-fluence UV-B response is also important because it confers adaptive advantages to crops under field conditions, where high-light intensity is often associated with water deficit (Gitz and Liu-Gitz, 2003).

The UV-B morphogenic response is regulated by a specific pathway that involves the *UV RESISTANCE LOCUS 8* (*UVR8*) gene (Kliebenstein et al., 2002; Brown et al., 2005; Favory et al., 2009). UVR8 is the photoreceptor of UV-B light (Rizzini et al., 2011; Christie et al., 2012; Wu et al., 2012) that is required for a UV-B-stimulated compensatory increase in epidermal leaf cell size, for normal progression of endoreduplication in response to UV-B, for stomatal differentiation and functions in plant acclimation, and for survival under solar UV (Wargent et al., 2009a, 2009b; Morales et al., 2012). At the transcriptional level, UVR8 regulates the expression of a range of genes involved in acclimation to and protection against UV-B radiation (Jenkins, 2009). Among them is the *ELONGATED HYPOCOTYL5* (*HY5*), a known regulator of photomorphogenesis in visible light (Chen et al., 2004), which is a key effector of the UVR8 signaling pathway (Ulm et al., 2004; Brown et al., 2005; Brown and Jenkins, 2008; Jenkins, 2009). The E3 ubiquitin ligase CONSTITUTIVELY PHOTOMORPHOGENIC1 (COP1) is also required for the activation of *HY5* gene expression under UV-B. In contrast with its repressor function in visible light-induced photomorphogenesis through the degradation of HY5 (Osterlund et al., 2000; Saijo et al., 2003), COP1 is a positive regulator of the UV-B response through interaction with the UVR8 photoreceptor (Oravecz et al., 2006; Cloix et al., 2012).

In an effort to identify plant genes involved in osmotic stress responses, an *Arabidopsis thaliana* (*Arabidopsis*) cDNA library was used to complement the lytic phenotype of the osmo-sensitive yeast mutant *mpk1 ppz1*. The *UVR8* gene was identified to be able to complement the growth defect of *mpk1 ppz1*. We also found that the expression of *UVR8* is up-regulated in *Arabidopsis* plants grown under salt or osmotic stress conditions. Furthermore, the ectopic expression of *UVR8* causes pleiotropic effects on plant growth, such as a general reduction of plant organ size, leaves with smaller cells, reduced root growth, and the accumulation of flavonoids, suggesting that, in the *UVR8*-overexpressing plants, grown under low levels of UV-B light, the UV-B morphogenic response is enhanced in comparison to the control plants. The growth defects of the *UVR8*-overexpressing plants were even more severe under osmotic and salt stress. In contrast, the inactivation of *UVR8* expression does not affect growth under standard or mild drought stress conditions, but enhances shoot growth under high-salt stress. We propose that UVR8 is a new component in the osmotic stress and UV-B plant crosstalk, with a key role in the reduction of plant vegetative growth under suboptimal environmental conditions.

RESULTS

UVR8 Complements the Lytic Phenotype of the Osmo-Sensitive *mpk1 ppz1* Yeast Mutant

With the aim to identify genes involved in hypo-osmotic stress signaling in plants, we used a cDNA library from *Arabidopsis* leaves (Minet et al., 1992) to transform a yeast mutant strain in which the *MPK1* and *PPZ1* genes were disrupted. The Mpk1/Slt2 MAP kinase is required to maintain cell integrity and the Ppz1 phosphatase plays an important role in the maintenance of K^+ and pH homeostasis. The lytic phenotype of the *mpk1 ppz1* double mutant is due to the combination of increased internal turgor pressure in Ppz1-deficient strains (because of K^+ overaccumulation) and cell wall instability in strains lacking MPK1 (Merchan et al., 2004). Thus, its growth requires the addition of an osmostabilizer, such as 1 M sorbitol (Lee et al., 1993).

To screen for *Arabidopsis* cDNA clones able to complement the lytic phenotype, the transformed yeast cells were plated on medium without sorbitol. The screen resulted in the identification of several independent clones that rescue the growth defect of the yeast *mpk1 ppz1* double mutant. Five

clones were redundant and all of them encoded full-length cDNA sequences corresponding to the *At5g63860* gene that encodes the UV-B photoreceptor UVR8 and regulates UV-B protection (Kliebenstein et al., 2002; Brown et al., 2005; Rizzini et al., 2011). The data for one representative clone are shown in Figure 1.

The increased tolerance to hypo-osmotic stress of the double mutant yeast strain *mpk1 ppz1* induced by *UVR8* overexpression suggests a putative role of *UVR8* in the plant's response to osmotic stress, besides its well-known involvement in the UV-B response.

UVR8 Expression Is Up-Regulated under Osmotic and Salt Stress

To investigate the involvement of *UVR8* in the response to abiotic stress, we analyzed its expression by real-time PCR (qRT–PCR), in *Arabidopsis* plants subjected to different environmental stimuli. Transfer of 2-week-old plants to Murashige and Skoog (MS) medium supplemented with NaCl (100 mM) or PEG (–0.5 MPa) for 24 h induced a 2.5-fold and 4.5-fold increase in the level of *UVR8* expression, respectively (Figure 2A). Also, transfer to starvation conditions (no sucrose, darkness) for 24 h slightly enhanced the level of *UVR8* expression. Exposure to UV-B light for 2 h did not significantly enhance *UVR8* expression (Figure 2A), in agreement with previous data (Tohge et al., 2011). Analysis of *UVR8* expression using the *Arabidopsis* eFP browser at BAR (Winter et al., 2007) and at Genevestigator (Hruz et al., 2008) confirmed that the expression of *UVR8* is slightly enhanced in response to various abiotic stress conditions (Supplemental Tables 1 and 2).

To further analyze the up-regulation of *UVR8* expression under salt or osmotic stress, an antibody directed against UVR8 was used to detect UVR8 protein levels in wild-type plants treated for 24 h with NaCl or PEG (as reported above). As shown in Figure 2B, in response to PEG-mediated osmotic stress, the levels of UVR8 were significantly higher, whereas no significant increase was observed in NaCl-treated plants.

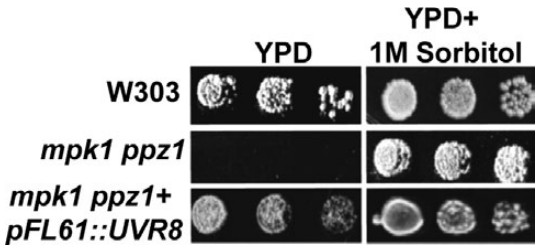

Figure 1. Complementation of *mpk1 ppz1* Double Mutants by *UVR8*. The indicated strains, wild-type (W303), *mpk1 ppz1*double mutant, and *mpk1 ppz1* transformed with the vector containing *UVR8* cDNA (PFL61-UVR8), were grown on selective medium containing 1 M sorbitol (SORB.), as described in the 'Methods' section, serially diluted in sterile water plus 1 M sorbitol, and spotted onto YPD plates or YPD plates containing 1 M sorbitol. Images were taken after 3 d of incubation at 37°C. Similar results were obtained in three separate experiments.

Phenotypic Analysis of *UVR8*-Overexpressing Plants

The observation that *UVR8* confers an enhanced tolerance to osmotic stress in yeast and it is transcriptionally responding to osmotic stress prompted us to test the effect of *UVR8* overexpression in *Arabidopsis*. Independent transgenic lines overexpressing the *Arabidopsis UVR8* gene under the control of the 35S CaMV promoter (*35S-UVR8*) were generated and T_2 plants containing a single insertion locus of the 35S-*UVR8* transgene were selected. Phenotypes of T_3 plants of two homozygous lines containing the 35S-*UVR8* transgene (lines 1 and 2) and expressing high levels of UVR8 (Supplemental Figure 1A) were analyzed and compared to those of the control plants transformed with the empty vector. Since similar phenotypic effects were observed for both transgenic lines, only the data for one line are presented.

Under standard growth-chamber fluorescent white light (80–90 μmol m^{-2} s^{-1}), containing low levels of UV-B (0.03 μmol m^{-2} s^{-1}), *35S-UVR8* plants, grown both *in vitro* and in soil, were smaller than control plants and showed many morphological changes (Figure 3). When grown *in vitro* under continuous light, hypocotyl and petiole length and cotyledon area of *35S-UVR8* seedlings were significantly reduced (Table 1). In addition, these plants visually accumulated more anthocyanins at the hypocotyls (Figure 3A), as already reported by Favory et al. (2009). The difference in stem height persisted at maturity, as it was decreased by 30% in the *35S-UVR8* plants compared to control plants (Table 1). The rosette diameter only reached 60% of that of the control (Figure 3B and Table 1).

To characterize in more detail the vegetative phenotype of the lines overexpressing *UVR8*, 21-day-old plants grown *in vitro* were harvested and their leaf area was measured at individual leaf positions. All leaves analyzed were significantly smaller than those of the control plants (Figure 3C and 3D). Detailed analysis of the first two leaves revealed that the decreased leaf area resulted from a reduction in leaf length and width (Figure 3F and 3H, and Supplemental Figure 2A and 2B). To understand whether the reduced leaf size observed in *35S-UVR8* plants was correlated with a reduction in cell number and/or in cell size, the lamina adaxial epidermis of the first two expanded leaves was analyzed. The number of the epidermal cells was unchanged in comparison to the control, whereas the mean cell size was significantly decreased (Figure 3H and Supplemental Figure 2C). Therefore, the observed leaf phenotype of the *35S-UVR8* plants was mainly the result of a reduction in cell expansion.

Plants overexpressing *UVR8* showed other notable alterations during development such as early flowering. Whereas long-day-grown (16-h light/8-h dark) control plants start flowering after the formation of approximately 13 rosette leaves, *35S-UVR8* plants flowered after producing 10 rosette leaves (Figure 3B). At maturity, *35S-UVR8* plants produced shorter siliques (Figure 3G) and the seed weight was 15% reduced compared to the control plants (Table 1).

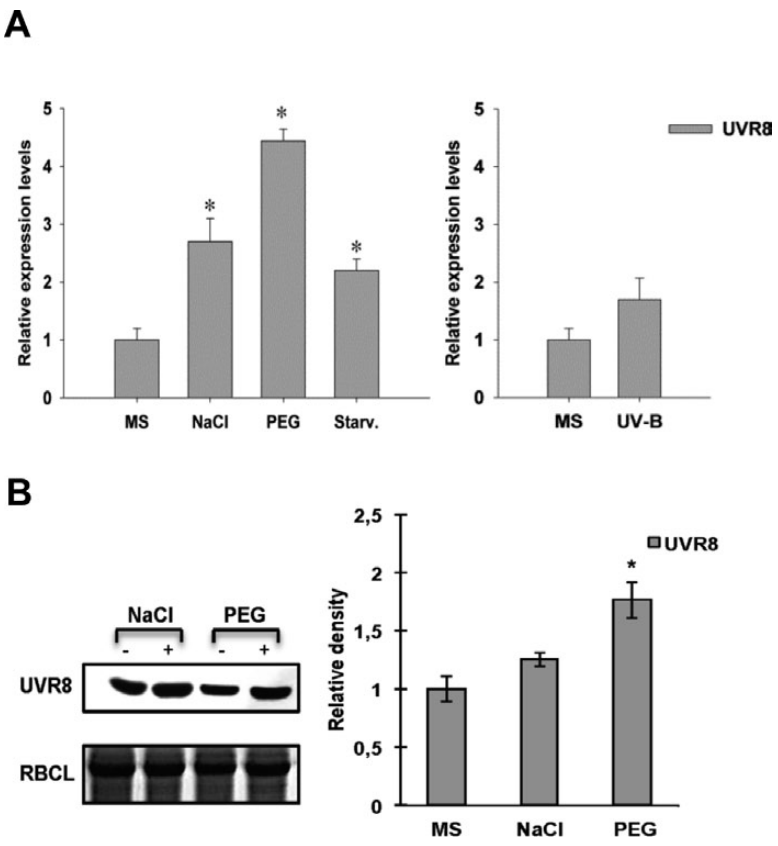

Figure 2. *UVR8* Expression under Abiotic Stress.

(A) *UVR8* mRNA expression in plants grown under normal conditions or upon exposure to abiotic stress. *UVR8* relative expression levels in 2-week-old plants grown *in vitro* on MS medium or after transfer for 24 h to medium supplemented with NaCl (100 mM) or PEG (–0.5 MPa); after transfer to starvation conditions (no sugar, dark); or after exposure to 5 μmol m^{-2} s^{-1} of UV-B light for 2 h. Relative transcript levels of *UVR8* were determined by qRT–PCR and the values were normalized to the untreated plants using 18S ribosomal RNA as an internal control. Data represent average of three independent experiments ± SD.

(B) UVR8 protein accumulation in wild-type plants after exposure to NaCl (100 mM) or PEG (–0.5 MPa) for 24 h. Plants were grown as reported above and UVR8 protein levels were analyzed by Western blotting with an anti-UVR8 antibody. The analysis was performed in triplicate and UVR8 relative protein levels were determined by densitometric analysis using Image J. The values were normalized to the untreated plants using rubisco large subunity (RBCL) and averages ± SD are shown ($n = 3$; $P < 0.05$).

Together, these data indicate that the ectopic expression of *UVR8* causes a general reduction of plant growth, mainly by the negative regulation of cell expansion.

Characterization of *35S-UVR8* Plants under Stress Conditions

The observed growth reduction in *35S-UVR8* plants is similar to the growth response of plants exposed to salt and osmotic stress. Therefore, we analyzed the response of *35S-UVR8* plants to severe or mild salt and osmotic stress conditions.

For severe stress treatment, plants were germinated on nylon mesh filters placed on MS medium and, after 2 weeks, transferred to medium supplemented with 150 mM NaCl or 200 mM mannitol. Under these stress conditions, the growth of the *35S-UVR8* plants was visibly more reduced than that of the control plants (Figure 4A). However, on medium supplemented with NaCl, the survival percentage of the *35S-UVR8* plants was similar to that of the control plants (46% versus 56%; Figure 4A), whereas, on medium supplemented with mannitol, it was significantly decreased (44% versus 68%; Figure 4A). Interestingly, when UV-B was filtered out from the light source, the phenotypes of the *35S-UVR8* plants grown on 200 mM mannitol were not different from those of the control plants (Figure 4B), suggesting that the sensitivity of the *35S-UVR8* plants grown on 200 mM mannitol and under low levels of UV-B was due to the combination of these two conditions.

We further analyzed the growth phenotype of the *35S-UVR8* plants upon mild stress conditions. To this end, plants were grown on MS medium supplemented with 50 mM NaCl or 25 mM mannitol—a condition that is not lethal but reduces growth (Skirycz et al., 2010). After 21 d, the leaf area was measured at individual leaf positions and percentages of rosette area reduction were calculated for the transgenic and the control plants. As shown in Supplemental Figure 3A, under low-salt or mannitol conditions, the control plants showed a reduction of 26% and 32%, respectively. Under salt

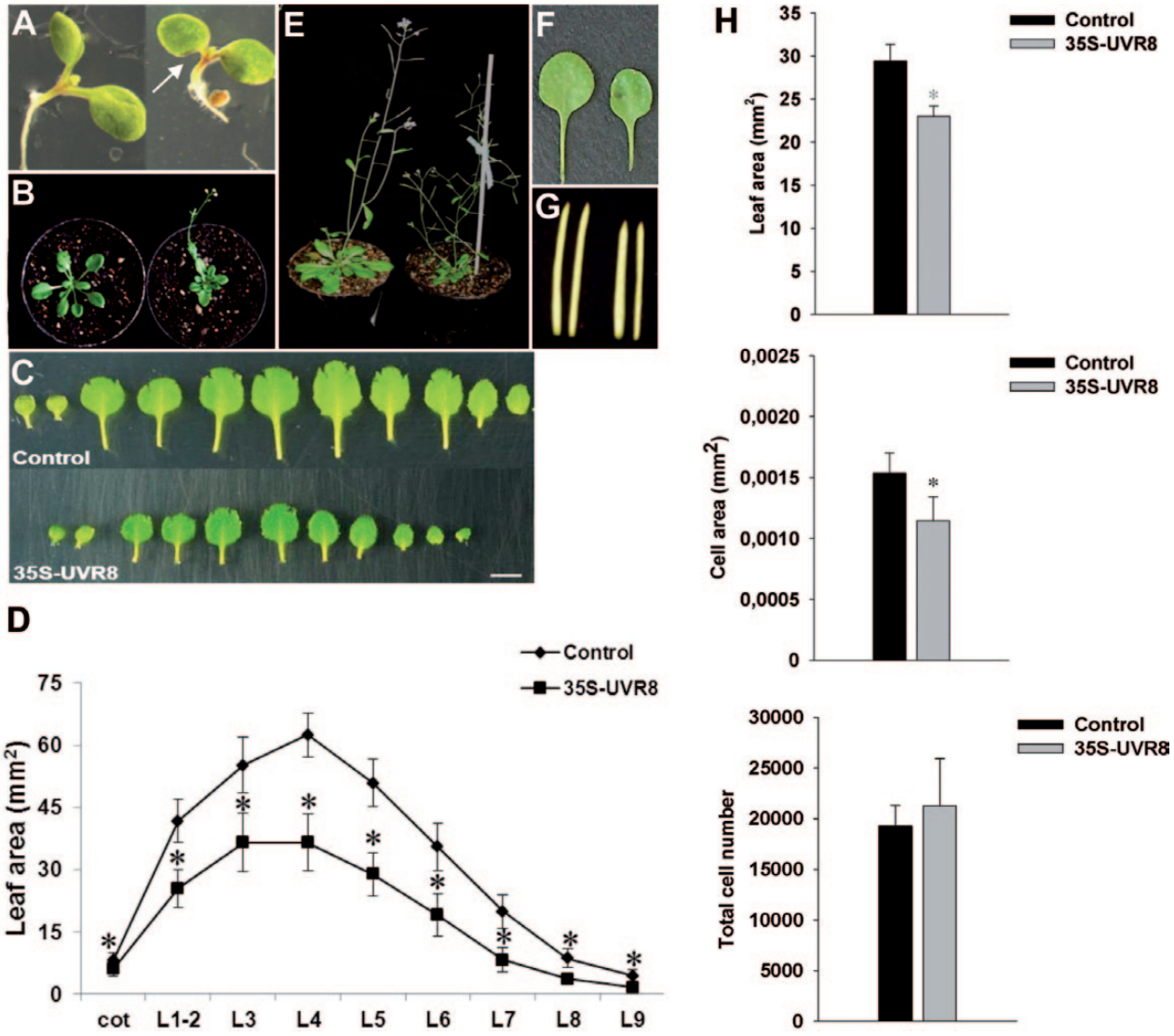

Figure 3. Phenotypic Characterization of *35S-UVR8* Plants.

(A) Seven-day-old seedlings overexpressing *UVR8* (right) as compared to control plants (left), grown *in vitro* at 23°C under a 16-h light/8-h dark photoperiod.

(B) Thirty-day-old *UVR8* transgenic plants (right) grown in soil. At this time, *UVR8*-overexpressing plants had already produced an inflorescence.

(C) Photographs of representative leaf series of *35S-UVR8* plants. Plants were grown *in vitro* at 23°C under a 16-h light/8-h dark photoperiod and leaf series (cotyledons on the left and youngest leaves on the right) photographed 21 d after sowing (DAS); bar = 10 mm.

(D) Area of rosette leaves at different positions. Values are averages ± SD (n = 14; * P = 0.05).

(E) Six-week-old control (left) and *35S-UVR8* (right) plants grown in soil.

(F) First leaves (leaf1–2) of 30-day-old control (left) and *35S-UVR8* (right) plants grown *in vitro*.

(G) Siliques of *35S-UVR8* (right) plants are visibly shorter than those of the control (left).

(H) Leaf measurements of 21-day-old *35S-UVR8* plants grown *in vitro*. To analyze the cellular basis of the size differences between the control and *35S-UVR8*, the leaf area, the epidermal cell number, and cell area were measured. Values are averages ± SD (n = 5; * P = 0.05).

stress, the reduction of the *35S-UVR8* plants was the same as that of the control plants (Supplemental Figures 2D and 3A), whereas, in the presence of mannitol, it was significantly increased (46%) (Supplemental Figure 3A). This sensitivity to the mannitol treatment was particularly observed in the younger leaves (Supplemental Figure 2E).

Above data indicate that the growth inhibition and morphogenic response triggered by *UVR8* overexpression in plants under low levels of UV-B was exacerbated by mannitol-induced osmotic stress, but not significantly affected by ionic stress.

Ectopic Expression of *UVR8* Results in an Increased *CHALCONE SYNTHASE* Expression and Flavonoid Accumulation

Consistently with previous data (Favory et al., 2009), *UVR8*-overexpressing plants displayed a higher tolerance to UV-B

Table 1. Phenotypical Analysis of *35S-UVR8* Plants.

Parameter	Control	*35S-UVR8*
Size		
Height (cm)[a]	31.6 ± 0.66	22.0 ± 0.72***
Rosette diameter (cm)[a]	7.5 ± 0.13	4.4 ± 0.2***
Cotyledon size (mm^2)[b]	3.8 ± 0.10	3.2 ± 0.07***
Hypocotyl length (mm)[b]	1.3 ± 0.03	1.0 ± 0.01***
Petiole length (mm)[b]	1.2 ± 0.02	0.8 ± 0.02***
Number		
Rosette leaves[c]	13.0 ± 0.27	10.1 ± 0.21**
Seeds weight (mg/plant)	31.2 ± 3.5	22.5 ± 6.47**

The bold case indicates the age of the plants used for the measurements. [a] 42-day-old plants grown in soil in a growth chamber at 23°C under a 16-h light/8-h dark photoperiod. [b] 7-day-old seedlings grown on continuous light on MS plates. [c] 30-day-old *35S-UVR8* plants grown in soil. At least 25 plants were used for the analysis. Data shown are averages ± SE; *** $P < 0.0001$; ** $P < 0.001$.

(83% of survival) compared to control plants (45% of survival; Supplemental Figure 3B). In addition, the expression level of *CHALCONE SYNTHASE* (*CHS*), encoding the first committed enzyme for flavonoid biosynthesis, was seven-fold increased in the *35S-UVR8* plants grown under low levels of UV-B (Figure 5A).

To further detail the activation of the flavonoid pathway upon *UVR8* overexpression, we measured the flavonoid content from leaves of *35S-UVR8* and control plants by HPLC-UV. Comparison of HPLC profiles at 345 nm showed that the accumulation of several flavonols in *UVR8*-overexpressing plants was higher than that in control plants (Figure 5B and 5C). Products were identified by the characteristic UV absorbance spectrum of their respective aglycones, and the nature of the glycosides was inferred from their mass spectrum. The main flavonol derivatives were kaempferol-3-O-[rhamnosyl (1>2) glucoside]-7-O-rhamnoside (K1), kaempferol-3-O-glucoside-7-O-rhamnoside (K2) and kaempferol-3-O-rhamnoside-7-O-rhamnoside (K3), and their structures are given in Figure 5D. The 345-nm absorption spectrum also showed a

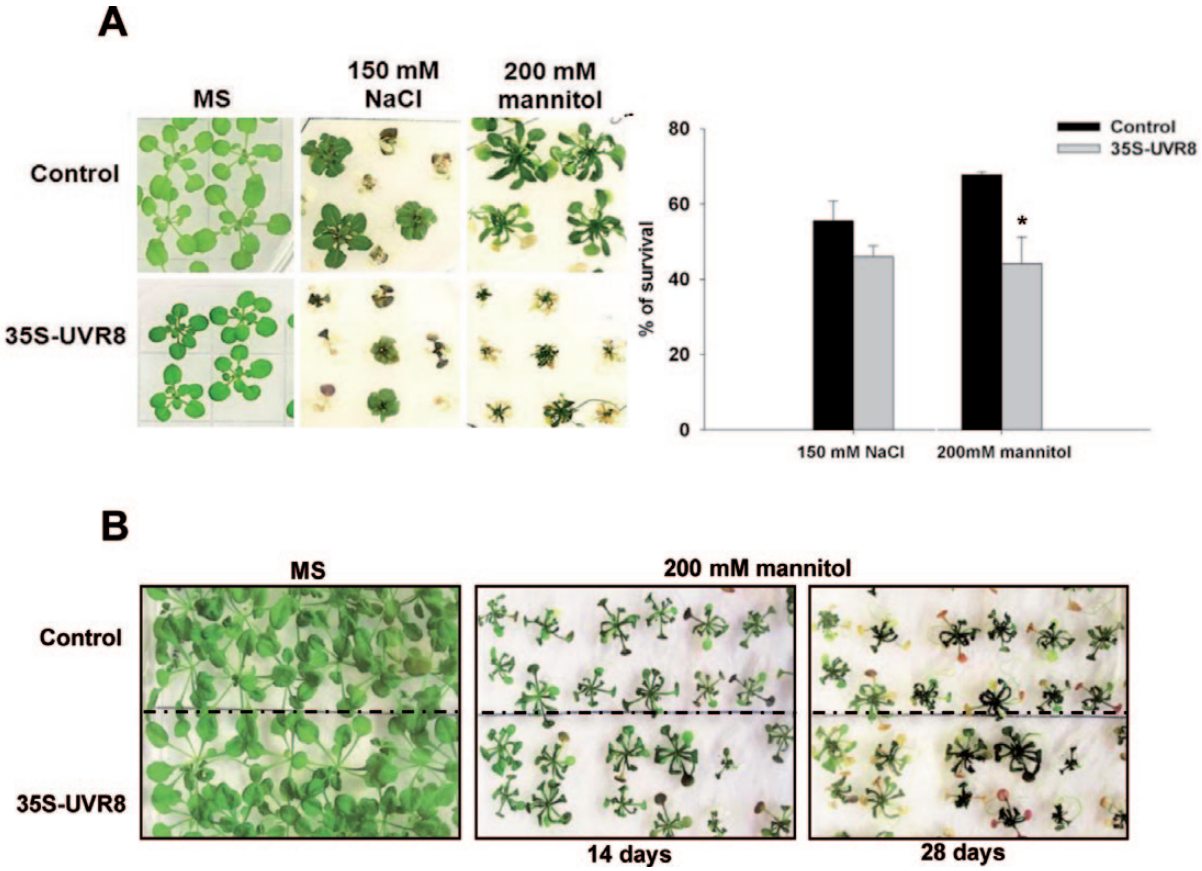

Figure 4. Response of *35S-UVR8* Plants to Severe Stress.

(A) Growth analysis on severe stress conditions. Plants were grown *in vitro* for 2 weeks on meshes placed on MS medium and transferred on MS media supplemented with NaCl (150 mM) or mannitol (200 mM). Plants were photographed after 3 weeks and the percentage of survival was recorded. The results are averages of two independent replicates (n = 70–80) ± SD.

(B) Phenotypes of *35S-UVR8* or control plants grown for 14 d and 28 d on 200 mM mannitol under mylar filter used to screen out the UV-B light.

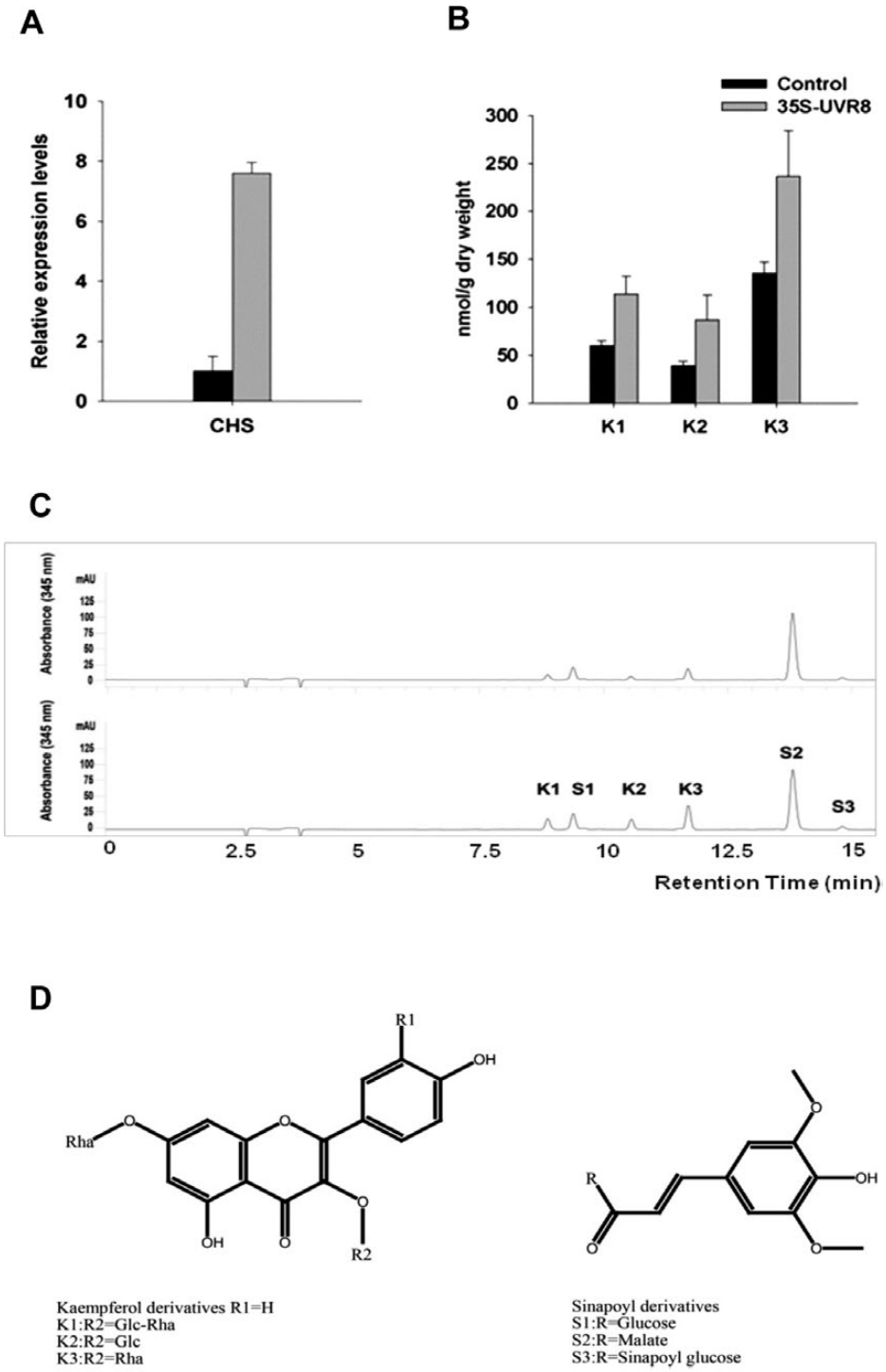

Figure 5. *CHS* expression and Analysis of Flavonoid Content in *35S-UVR8* Plants.

(A) Accumulation of *CHS* mRNA in 7-day-old transgenic *UVR8*-overexpressing seedlings grown under low levels of UV-B. Relative transcript levels of *UVR8* were determined by qRT–PCR and normalized using *ACT2* as internal control. Error bars represent standard deviations of three replicates.
(B) Levels of flavonols accumulating in leaves of *35S-UVR8* plants compared to control plants. The main flavonol derivatives were kaempferol-3-O-[rhamnosyl (1>2) glucoside]-7-O-rhamnoside (K1), kaempferol-3-O-glucoside-7-O-rhamnoside (K2) and kaempferol-3-O-rhamnoside-7-O-rhamnosiden (K3). The values are expressed as nmol g^{-1} dry weight. Mean values and standard deviations are given for three replicates.
(C) HPLC of soluble phenolics extracted from *35S-UVR8* plants grown in soil for 5 weeks. Profile of *UVR8* transgenic extracts compared to control plants, at 345 nm. The sinapoyl derivatives were sinapoyl glucose (S1), sinapoylmalate (S2), and disinapoylglucose (S3).
(D) Structure of flavonol glycosides and sinapoyl derivatives were inferred from their mass spectral properties.

major peak, which corresponds to sinapoylmalate (S2), but its accumulation was unchanged in *35S-UVR8* or control plants (Figure 5C and 5D).

Therefore, under low levels of UV-B, the ectopic expression of *UVR8* activates *CHS* transcription and flavonoid biosynthesis.

UVR8 Overexpression Reduces Root Growth and Alters Root Development

The negative effect of *UVR8* overexpression on vegetative growth prompted us to analyze the effects of its ectopic expression on root development. The primary root length of 7-day-old *UVR8*-overexpressing seedlings was 18% reduced in comparison to the control (Figure 6A and Table 2). To investigate the cellular basis of the size decrease associated with high levels of UVR8 protein, the meristem size in 7-day-old roots was analyzed by counting the number of cortex cells starting from the quiescent center to the beginning of the elongation zone. Compared to the control plants, the cell number in *35S-UVR8* plant root meristems was unchanged (Table 2), suggesting that the inhibition of root elongation observed in the primary root of *35S-UVR8* seedlings is mainly caused by a reduced cell expansion. A reduction of primary root length (13%) and lateral root density (60%; number of emerged lateral roots cm^{-1} primary root) was also seen in 14-day-old *35S-UVR8* seedlings (Figure 6B and Table 2). We also noticed that the lateral roots of the *UVR8*-overexpressing plants were mainly localized in the bottom part of the branching zone of the root (Dubrovsky et al., 2011; Dubrovsky and Forde, 2012) (Figure 6B). To analyze this phenotype, we divided the primary root in two equal parts (bottom and upper, Figure 6B) and counted the number of lateral roots. We found that the number of lateral roots of the *UVR8*-overexpressing plants was smaller in the upper part in comparison to the control (63% versus 77%), whereas, in the bottom part, it was significantly increased (37% versus 23%; Figure 6C). To explain the defects observed in the lateral root development of *35S-UVR8* plants, the number of lateral root primordia (LRPs) and developmental stages of LRP were analyzed. We found that the number of LRPs and emerged lateral roots was 12% and 68% reduced in comparison to the control, respectively. An increased number of LRPs in the stages V and VI was found in the root of the *UVR8*-overexpressing plants (Figure 6D and Table 2). Together, these data indicate that the reduced lateral root number of the *UVR8*-overexpressing plants is mainly due to defects in lateral root emergence, since the LRP initiation is less affected.

The defects observed in *35S-UVR8* plants during root development suggest that auxin transport might be altered (Casimiro et al., 2001; Bhalerao et al., 2002; De Smet and Jürgens, 2007). Since the vegetative shoot of *UVR8*-overexpressing plants has increased levels of flavonoid and because flavonoids are endogenous regulators of auxin transport (Taylor and Grotewold, 2005), we analyzed the accumulation of flavonoids in the root of *35S-UVR8* seedlings by using the flavonoid-specific dye diphenylboric acid 2-aminoethyl ester (DPBA). The intensity of fluorescence, quantified by Image J, was found to be 2.2-fold increased in the *UVR8*-overexpressing plants in comparison to the control, indicating a higher flavonoid content (Figure 6E).

Taken together, these data suggest that the ectopic expression of *UVR8* reduces and alters root growth. The root phenotype of the *35S-UVR8* plants could be associated with enhanced flavonoid levels.

Phenotypes of the *uvr8-6* Mutant under Normal and Stress Conditions

To further investigate the putative role of *UVR8* in the regulation of cell expansion and the responses to osmotic and salt stress, we analyzed the T-DNA-tagged *uvr8-6* mutant. The T-DNA was inserted in the ninth intron of the *UVR8* gene (Favory et al., 2009) and Western blot analysis showed the complete absence of UVR8 protein (Supplemental Figure 1B).

We first analyzed the effect of UVR8 inactivation on vegetative growth by measuring the cotyledon area, and petiole and hypocotyl lengths. When grown in continuous white light conditions, cotyledon area and petiole length of the 7-day-old mutant seedlings were slightly increased in comparison to the wild-type plants (Supplemental Table 1). The hypocotyl length was similar to that of the control, as previously described (Favory et al., 2009) (Supplemental Table 1).

The leaf area of the *uvr8-6* plants, either grown on MS or upon mild stress conditions induced by 50 mM NaCl or 25 mM mannitol, was similar to that of the control plants (Supplemental Figure 4A–4D).

We next investigated the effect of UVR8 inactivation on leaf growth under severe stress conditions. When the *uvr8-6* plants were grown on mesh filters laid on MS medium for 2 weeks and then transferred to medium containing 150 mM NaCl, the percentage of survival was 16% greater than that of the control plants (44% versus 28%) and the rosette area was 20% increased (Figure 7). Under salt-stress conditions, the leaf areas of the *uvr8-6* plants measured at individual leaf positions were, for most of the leaves, significantly larger than those of the control plants (Supplemental Figure 5A). On a medium supplemented with 200 mM mannitol, the survival of *uvr8-6* plants was not different from that of the wild-type plants (48% versus 49%; Supplemental Figure 5B). Furthermore, to ascertain whether or not the salt-stress response was UV-B dependent, severe salt stress was imposed on wild-type and *uvr8-6* mutant plants in the presence or absence of UV-B light. Wild-type and *uvr8-6* mutant plants were grown under low levels of UV-B or under mylar filters (used to screen out the UV-B) for 2 weeks on MS medium and then transferred to MS supplemented with 150 mM NaCl. In the absence of UV-B and upon exposure to 150 mM NaCl, there were no differences in the phenotype and percentage of survival of the wild-type and *uvr8-6* plants. In the presence of UV-B, the wild-type plant was more sensitive to NaCl treatment compared to the *uvr8-6*

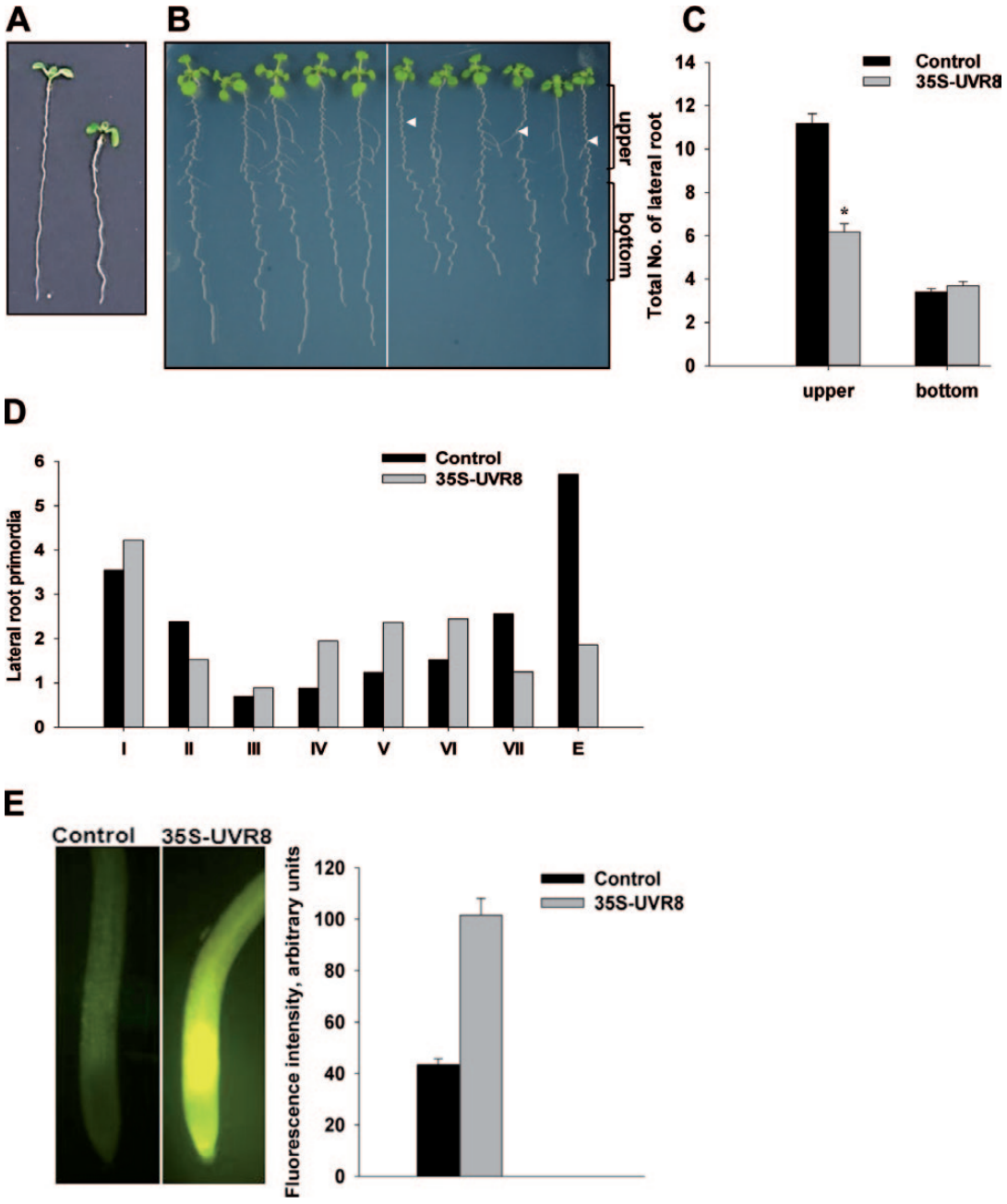

Figure 6. Root Phenotypes of *35S-UVR8* Plants.

(A) Seven-day-old *35S-UVR8* seedlings (right; control plant on the left) grown *in vitro* in a growth chamber at 23°C under continuous light.

(B) Fourteen-day-old *35S-UVR8* plants (right, control plants on the left) grown *in vitro.* The arrow head indicates the bottom part of the branching zone of the root.

(C) Lateral root distribution in different sections of roots (as indicated in (B)) of 14-day-old *35S-UVR8* plants. Data are averages ± SE (n = 20).

(D) Detailed staging of the root. Data are averages (n = 8–12).

(E) DPBA-visualized flavonol accumulation in 7-day-old *35S-UVR8* seedlings compared to the control and fluorescence intensity calculated by ImageJ. Data are averages ± SE (n = 12–16).

mutant (Figure 7B), indicating that this negative additive response requires *UVR8*.

To understand the role of UVR8 on root development, we analyzed the root phenotype of the *uvr8-6* mutant. The plants were grown on medium containing 1.5% sucrose under continuous light and were examined for several parameters including primary root length, number of root primordia, and lateral root density (Supplemental Table 1). In these growth conditions, the root growth of the *uvr8-6* mutant was similar to that of the wild-type plants. Similar results were obtained

Table 2. Morphological Comparison of the Root of the Control and *35S-UVR8* Plants.

Parameter	Control	*35S-UVR8*
Primary root length (mm)[a]	25.0 ± 0.30	20.5 ± 0.28*
Cortex cells (no.)[a]	27.2 ± 0.50	28.2 ± 0.90
Total primordia (no.)[a]	156	138
Primary root length (cm)[b]	7.0 ± 0.12	6.1 ± 0.13**
Lateral root density (no./cm)[b]	2.1 ± 0.04	0.85 ± 0.12**
Lateral root length (cm)[b]	1.95 ± 0.05	2.12 ± 0.05

The bold case indicates the age of the plants used for the measurements. [a] 7-day-old seedlings grown on continuous light on MS plates. [b] 14-day-old seedlings grown on continuous light on MS plates. At least 25 plants were used for the analysis. Data shown are averages ± SE; *** $P < 0.0001$; ** $P < 0.001$.

when the plants were grown under a 16-h light/8-h dark photoperiod (Supplemental Figure 5C and Supplemental Table 2).

We also analyzed the flavonoid content of *uvr8-6* mutant roots by DPBA staining and the intensity of fluorescence was similar to that of the control plants (Supplemental Figure 5D), suggesting that the absence of *UVR8* does not affect flavonoid accumulation in the root.

Together, these data indicate that the *uvr8-6* plants showed a normal development under either standard conditions or mild osmotic stress conditions, whereas, under strong salt stress, their growth was less affected than that of control plants.

Auxin Content in the *35S-UVR8* or *uvr8-6* Mutant Plants

The proposed role for auxin in the UV-B-mediated morphogenic response (Hectors et al., 2012) together with

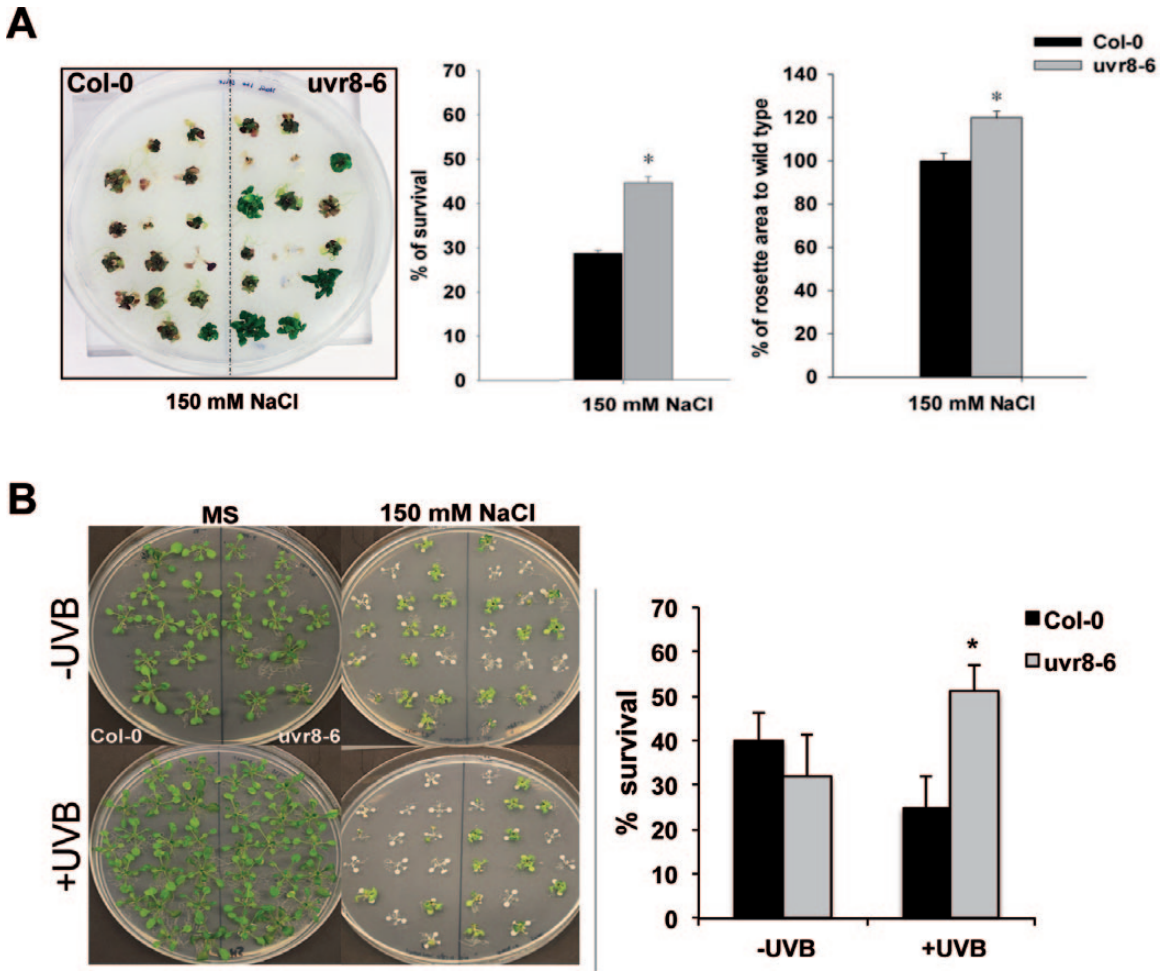

Figure 7. Response of *uvr8-6* Plants to 150 mM NaCl.

(A) Response of the *uvr8-6* mutant to severe stress under low levels of UV-B. Plants were grown *in vitro* for 2 weeks and then transferred to MS medium supplemented with NaCl (150 mM). Plants were photographed after 3 weeks on stress conditions and the percentage of survival (on the left) and the percentage difference of rosette size upon salt stress (on the right) were recorded. Survival rates and SD were calculated from the results of three independent experiments ($n = 80$ plants/genotype).

(B) Phenotypes and response of the *uvr8-6* mutant to severe stress under low levels of UV-B or under mylar filters used to screen out the UV-B light. Plants were grown as above and were photographed after 1 week on stress conditions and the percentage of survival was scored. Data are averages ± SD ($n = 90$).

the observed growth phenotypes of the *35S-UVR8* plants prompted us to analyze the levels of endogenous auxin in *35S-UVR8* or in *uvr8-6* mutants. To this end, the levels of IAA and IAA conjugates were measured in old and young leaves of 21-day-old plants or in the root of 7-day-old seedlings grown *in vitro* under white light conditions. The levels of free IAA as well as IAA conjugates were not significantly different in all the samples analyzed (Supplemental Figures 6 and 7), but we observed a tendency, in the content of the IAA conjugates, to decrease in the *UVR8*-overexpressing plants and to increase in the *uvr8-6* mutant. These data suggest that the role of auxin in the UV-B morphogenic response could be *UVR8*-mediated.

DISCUSSION

UVR8 Is Up-Regulated by Osmotic Stress and Its Ectopic Expression Affects Plant Growth

In a natural environment, plants have to cope with combinations of various stresses. For example, water deficit imposes osmotic stress on plants and is often associated to environments with an excess of radiation (light, UV-B). To overcome these unfavorable conditions, plants have evolved several adaptive responses that are in common between osmotic stress and UV-B light (reviewed by Gitz and Liu-Gitz, 2003). Among them, the reduction of plant growth is one of the major causes for crop yield reductions. This response is strictly controlled at cellular, molecular, and metabolic levels by complex networks involving different regulatory pathways, which are still far from being elucidated. We have found that the *UVR8* gene, a known regulator of plant morphogenesis under UV-B (Favory et al., 2009), was able to complement the lytic phenotype of the *mpk1 ppz1* osmo-sensitive mutant strain of *Saccharomyces cerevisiae*. Although we have no further evidence on its contribution in alleviating cell wall instability in the yeast mutant, other genes involved in the UV-B response have been identified previously by complementing the yeast osmo-sensitive calcineurin mutant, such as the gene encoding the *Arabidopsis* SALT TOLERANT (STO/BBX24) protein (Lippuner et al., 1996), which only later was shown to be involved in the UV-B signaling in plants (Jiang et al., 2009). A putative involvement of the *UVR8* gene in the plant's response to osmotic stress was also supported by the four-fold up-regulation of *UVR8* transcript and protein level in *Arabidopsis* plants upon PEG treatment and more slightly by NaCl. These data are consistent with microarray data publicly available at the *Arabidopsis* eFP browser at BAR (Winter et al., 2007) and at Genevestigator (Hruz et al., 2008) that showed a slight up-regulation of *UVR8* upon osmotic or salt stress. Interestingly, it has been reported that a barley variety that performed better in open field drought tests has a higher level of *UVR8* transcripts compared to a drought-sensitive cultivar (Guo et al., 2009). Finally, the expression of several genes involved in salt stress (*JR1*, *At1g16850*, *AOC3*, and *ANNAT1*) was found to be down-regulated in the *uvr8-6* mutant grown under solar UV, compared to the wild-type (Morales et al., 2012). Altogether, our data and these previous published results support a putative role of *UVR8* in the plant's response to osmotic stress, besides its well-known involvement in the UV-B response.

Elucidation of the interaction between osmotic stress and UV-B stress and their effects on plant growth and development would help in understanding the mechanism responsible for plant adaptation to changing environmental conditions in open fields. We have, therefore, generated *UVR8*-overexpressing transgenic lines that, grown under low levels of UV-B, showed shorter petioles, reduction of leaf and rosette expansion, decreased root growth, and a higher content of flavonoids than the control plants. The morphological and metabolic changes induced by *UVR8* overexpression were also seen in wild-type plants exposed to low levels of UV-B (Jansen, 2002; Potters et al., 2009; Hectors et al., 2010, 2012), suggesting that *Arabidopsis* plants with a higher level of the UVR8 protein have an enhanced photomorphogenic response, as already to some extent reported by Favory et al. (2009).

Cell Expansion Inhibition Causes Growth Defects in *UVR8*-Overexpressing Plants

The UV-B-induced reduction in plant growth, and more specifically in leaf area, has been attributed either to cell division or cell expansion or a combination of both (Jansen, 2002 and references herewith). We have demonstrated that the observed reduction in rosette leaf size in *UVR8*-overexpressing plants, grown under low levels of UV-B (0.03 μmol m^{-2} s^{-1}), was due to the inhibition of epidermal cell expansion. These data are consistent with the reduction in leaf size of *Arabidopsis* plants exposed to UV-B light that has been associated to the decreased cell expansion of the adaxial epidermal cells (Hectors et al., 2010). It has to be emphasized that, under low doses and/or chronic UV-B treatment, both reductions and increases in cell expansion and cell division have been reported, indicating that the effects of UV-B on cellular growth are controversial and probably due to differences in experimental conditions used (Hectors et al., 2010 and references herewith). Interestingly, the defect in cell expansion was observed also in the root systems of *UVR8*-overexpressing plants. The primary root and lateral root densities of *35S-UVR8* plants were 13% and 60%, respectively, reduced compared to the control plants, indicating that lateral root growth was most hampered. In *Arabidopsis*, lateral roots originate from pericycle cells, in a two-step process. First, lateral root initiation starts with the division of the pericycle cells and is regulated by auxin originating from the root tip (Casimiro et al., 2001; De Smet and Jürgens, 2007). Then, lateral root emergence is mainly driven by cell expansion and is depending exclusively on shoot-derived auxin (Bhalerao et al., 2002). The number of LRPs and emerged lateral roots of the *35S-UVR8* plants was 12% and 68%, respectively, reduced in comparison to that of the control plants. Although we

cannot exclude that these modifications in root architecture might be due to a pleiotropic effect of shoot reduction, the overall phenotype of the *UVR8*-overexpressing plants is reminiscent of auxin mutants (Zhao, 2010).

UVR8-Dependent Flavonoid Accumulation and Disturbance of Auxin Homeostasis

A growing body of evidence suggests that flavonoids may act as non-essential auxin transport inhibitors and that the UV-B-induced accumulation of flavonoid aglycones may affect polar auxin transport and hence plant architecture (Jansen, 2002; Peer and Murphy, 2007). In *35S-UVR8* plants, the leaf levels of kaempferol-3-O-rhamnoside-7-O-rhamnoside were 1.5 times higher in comparison to those in the control plants and, in the root, flavonoid levels were more than 50% increased. Mutations in genes that induce an accumulation of flavonoids or in genes encoding enzymes or transcription factors involved in the flavonoid biosynthesis cause dwarf phenotypes and root growth defects due to alterations in auxin transport or signaling (Sibout et al., 2006; Buer and Djordjevic, 2009; Grunewald et al., 2012). Thus, flavonoid accumulation, due to transcriptional *UVR8*-mediated activation of *CHS* and, possibly, due to other biosynthetic genes of the flavonoid pathway, in turn affecting auxin homeostasis, might contribute to the phenotype of the *UVR8*-overexpressing plants.

Interestingly, it has been reported that mutations in several genes involved in the *de novo* tryptophan-dependent auxin biosynthesis pathway, such as *NIT1* or *NIT3*, caused altered flavonoid accumulation, and an altered morphogenic response when exposed to UV-B, suggesting that UV-B-induced morphological responses may be affected by crosstalk between flavonoid accumulation and auxin homeostasis (Hectors et al., 2012). Although direct measurement of IAA and IAA conjugates in *UVR8*-overexpressing plants or *uvr8-6* mutants did not reveal significant differences (except for somewhat higher levels of IAA conjugates in the older leaves of *uvr8* mutant plants), all above observations suggest that the crosstalk between flavonoids and auxins may also be linked to UVR8 signaling.

UVR8 and Plant Long-Term Response to Osmotic Stress under Low Levels of UV-B

It has been reported that the UV-B-induced morphogenic response confers adaptive advantages under conditions associated with high-light environments and water stress and that *Arabidopsis* plants grown under UV-B light are more tolerant to drought stress (Gitz and Liu-Gitz, 2003; Poulson et al., 2006). Conversely, other studies showed that combined treatments of drought and UV-B interact, causing additive negative effects on growth of *Arabidopsis* wild-type plants, following exposure, as well as of other species (Comont et al., 2012 and references herewith). Such contrasting responses support a crosstalk between UV-B light and osmotic stress, but also highlight the need for further studies of this complex interaction. Our data demonstrated that effects of mild osmotic stress induced by a low concentration of mannitol, combined with a low UV-B level, affected negatively and in an additive manner the vegetative growth of *35S-UVR8* plants. This additive growth inhibition was mainly observed upon mannitol treatment, rather than NaCl-mediated ionic stress. Restraint of shoot growth has been regarded as an advantage to promote plant survival under adverse environmental conditions (Achard et al., 2006). Therefore, it might be expected that *UVR8*-overexpressing plants were more tolerant to severe osmotic stress. In contrast, under our experimental conditions, they were more sensitive, as was shown from the reduced percentage of survival upon 200 mM mannitol. The reduction in size of plant organs, frequently observed upon exposure to severe osmotic stress, can be largely attributed to the decreased cell expansion (Jaleel et al., 2009). Therefore, the impaired cell expansion of the *UVR8*-overexpressing plants might negatively affect their ability to regulate osmotic pressure and water uptake that, in turn, might be translated in an additional reduction in plant growth.

In addition to the defect in shoot growth expansion, the *UVR8*-overexpressing plants have also a reduced root system growth and alterations in their root architecture, which could aggravate their performance under osmotic stress. It has been largely proved that a more extensive root system is considered as a drought-avoidance strategy to improve the water and nutrients uptake when their availability in the soil is limited (Fukai and Cooper, 1995; Liao et al., 2001; Sharp et al., 2004). However, under low levels of UV-B, a growth phenotype reciprocal to the one observed in *35S-UVR8* plants was not detected in the *uvr8-6* null mutant plants, either in absence of stress or upon mannitol treatment. This suggests that the hypersensitive response to osmotic stress of the *35S-UVR8* plants is strictly UVR8-dependent.

Interestingly, the *35S-UVR8* plants exposed to severe osmotic stress and in absence of UV-B light could grow to the same extent as control plants. It was already reported that UV-B light is necessary for UVR8 function. Absorption of UV-B through UVR8 induces instant monomerization of the protein and its nuclear translocation to initiate expression of genes concerned with UV protection, such as *HY5* and *CHS*, with concomitant flavonoid production (Favory et al., 2009; Rizzini et al., 2011; O'Hara and Jenkins, 2013). Drought has also been associated with anthocyanin accumulation in various tissues, and flavonoid concentration was found significantly higher in combined stress-treated plants than in those treated with UV-B alone (Hughes et al., 2010; Comont et al., 2012). Under low levels of UV-B, the *UVR8*-overexpressing plants accumulated more flavonoids than control plants and the osmotic stress, simultaneously with the UV-B exposure, could further enhance the levels of UVR8 protein. This, in turn, could increase the content of flavonoid at higher levels and exacerbate the negative response on plant growth and survival.

To better understand the role of the *UVR8* gene in response to osmotic stress, we also analyzed the response

of the *uvr8-6* mutant under normal or stress conditions. In absence of osmotic stress and under low levels of UV-B (0.03 μmol m^{-2} s^{-1}), the growth of the *uvr8-6* plants was similar to that of the wild-type. In contrast, in response to high salt (150 mM NaCl) and under low levels of UV-B, the shoot growth of the *uvr8-6* plants was less inhibited and their survival percentage was higher than that of the control plants, whereas, under mylar filters, their phenotype and percentage of survival were similar. These data suggest that the increase in leaf area observed in the *uvr8-6* mutant plant under low levels of UV-B and salt stress (150 mM NaCl) is due to the combined conditions. This finding, together with the severe inhibitory effect of cell expansion induced by the ectopic expression of *UVR8*, indicates that UVR8 is required for the regulation of shoot growth reduction induced by low UV-B light and osmotic stress. Furthermore, the finding that the tolerance of the Col-0 plants to severe salt stress was significantly reduced under low levels of UV-B (whereas, without UV-B, it was similar to that of the *uvr8-6* mutant) suggests that UV-B light has a negative role in the tolerance of wild-type plants to severe osmotic stress and this response could be UVR8-mediated. Interestingly, it has been reported that UV-B light induces stomatal differentiation through UVR8, and that the *uvr8-6* mutant, grown under UV-B light, has a stomatal density lower than that of the wild-type plants, whereas, in absence of UV-B, it was similar (Wargent et al., 2009a). Thus, the reduced density of stomata could be associated with a reduced transpiration rate and contribute positively to sustain plant growth and survival of the *uvr8-6* plants. This also explains the reduced sensitivity of wild-type plants to salt stress when grown under low levels of UV-B.

The salt-tolerant phenotype of the *uvr8-6* plants could be also associated with a somewhat higher content of IAA conjugates found in the old leaves of the mutant plants in absence of stress. Increased levels of IAA conjugates were also found in drought-tolerant transgenic plants in response to water deficit, suggesting a role of auxin homeostasis in the acclimation response to this stress condition (Park, 2007; Park et al., 2007; Zhang et al., 2009).

Taken together, these data suggest again a possible crosstalk between UV-B light and osmotic stress response through UVR8, but further experiments are needed to uncover the role of UVR8 in this complex interaction.

UVR8 Is a New Putative Component in the Crosstalk between Osmotic and UV-B Stress

In the open field, crop plants are likely to experience multiple environmental stresses, which, when occurring simultaneously, can impact dramatically plant growth and development and, ultimately, yield. The plant molecular responses to abiotic stresses involve interactions with many molecular pathways and elucidation of these complex crosstalks is critical for crop improvement under limiting environmental conditions (Atkinson and Urwin, 2012).

The finding that UVR8 is involved in the osmotic stress response supports previous observations of the existence of a crosstalk between UV-B and osmotic stress (Gitz and Liu-Gitz, 2003; Poulson et al., 2006). It has been demonstrated that, in *Arabidopsis*, UVR8 interacts with COP1 to regulate the response to UV-B in a pathway that involves HY5 (Brown and Jenkins, 2008; Favory et al., 2009). HY5 has also been shown to have a role in the integration of light and abscisic acid signaling in seeds and seedlings by binding to the *ABI5* promoter (Chen et al., 2008). Interestingly, the *Arabidopsis* SALT TOLERANT STO/BBX24 protein interacts *in planta* with COP1 and HY5, but not with UVR8, regulating negatively the UV-B signaling (Jiang et al., 2012). HY5 also interacts with RADICAL INDUCED CELL DEATH1 (RCD1), another negative regulator of UV-B response (Jiang et al., 2009), which interacts with the plant Na^+/H^+ antiporter SOS1 (Katiyar-Agarwal et al., 2006). Altogether, these results uncover an extensive and complex network of key proteins, of which UVR8 is a component, with a crucial role in regulating plant morphological changes in response to multiple environmental stresses.

METHODS

Arabidopsis cDNA Library Screening and Complementation of Yeast Mutation

Yeast competent cells of *S. cerevisiae* (LY193 W303–1A *ppz1*::*TRP1 mpk1*::*LEU2*) (Merchan et al., 2004) were transformed with a cDNA library from *Arabidopsis* leaves, cloned in the expression plasmid pFL61 (Minet et al., 1992) by the LiCl transformation method (Ito et al., 1983). About 10^6 yeast transformants were screened for osmo-tolerance in plates with minimal medium (SD) without sorbitol. Putative positive colonies were then rescreened on YPD plates. Plasmid DNA was isolated from the yeast cells, characterized, and reintroduced into the original yeast mutant strain to confirm the complementation. For the drop test, yeast cells were grown on synthetic medium (SD) supplemented with 1 M sorbitol overnight and counted (after brief sonication) in the Particle Count and Size Analyzer, model Z2 (Coulter Inc.). The same amount of cells (2×10^6 cell ml^{-1}) was spotted on YPD plates. Complete medium contained 2% glucose, 2% peptone, and 1% yeast extract (YPD). Where indicated, YPD was supplemented with the indicated concentrations of sorbitol. Synthetic medium (SD) contained 2% glucose, 0.7% yeast nitrogen base (Difco) without amino acids, 50 mM MES [2-(*N*-morpholino)ethanesulfonic acid] adjusted to pH 5.5 with Tris, and the amino acids and purine and pyrimidine bases required for the strains.

Plant Material and Growth Conditions

A. thaliana ecotype Columbia (Col-0) and the T-DNA mutant *SALK_33468* (*uvr8-6*) were used in this study. Seeds of the *uvr8-6* mutant were generously provided by Roman Ulm (University of Geneve, Switzerland).

Plants were grown *in vitro* in half-strength MS medium (Murashige and Skoog, 1962), supplemented with 1% Sucrose and 0.5 g L^{-1} MES under a 16-h day (110 µmol m^{-2} s^{-1}), using fluorescent lamps (Spectralux Plus NL-T8 36W/840, *CP* LIGHTING, United Kingdom) and 8-h night regime. The UV-B light (0.03 µmol m^{-2} s^{-1}) emitted was measured by the SpectroSense2+ meter (Skye Instruments Ltd, United Kingdom) equipped with an SKU 430/SS2 UVB sensor.

Phenotypic Analyses

For shoot phenotyping, seedlings were grown on MS medium under continuous light (50–70 µmol m^{-2} s^{-1}). Images of the shoots were taken under a binocular microscope (Leica) and measurements (cotyledon area, petiole length, and hypocotyl length) were made using the NIH Image 1.62 software.

For rosette leaf area measurements, 14 seedlings were grown under *in vitro* conditions for 21 d. Individual leaves (cotyledons and rosette leaves) were dissected, and their area was measured with the ImageJ software (http://rsb.info.nih.gov/ij/, accessed 31 January 2013). For the leaf area analysis, the first and second leaves were harvested from 8–10 plants grown *in vitro*. The leaves were cleared with 100% ethanol, mounted in lactic acid on microscope slides, and photographed. The leaf area was determined with the ImageJ software (http://rsb.info.nih.gov/ij/, accessed 31 January 13). Abaxial epidermal cells were analyzed as reported by Gonzalez et al. (2010).

To characterize root growth, plants were grown on vertical square plates with solid half-strength MS medium. The plates were incubated, depending on the experiments, under continuous light or night/day conditions, as described above. For the analysis of the root growth of the *uvr8-6* mutant, seeds were also plated on medium consisting of 1 MS salts, pH 6.0, 0.8% (w/v) agar, 1.5% (w/v) sucrose, 1.0 µg ml^{-1} thiamine, 0.5 µg ml^{-1} pyroxidine HCl, and 0.5 µg ml^{-1} nicotinic acid as reported by Brown et al. (2001). Root length, lateral root length, and the number of lateral roots were measured from digital images of the plates using the NIH Image 1.62 software.

To count LRPs and for lateral root staging, seedlings were treated as reported by Malamy and Benfey (1997). Roots were mounted in 50% glycerol on glass microscope slides and viewed with an Olympus BX51 microscope equipped with DIC optics.

Stress Treatment

For growth analysis on mild stress conditions, seeds were sown on MS medium or MS medium supplemented with either 25 mM mannitol or 50 mM NaCl, and grown under a 16-h day/8-h night regime, in 110 µmol m^{-2} s^{-1} white light and 0.03 µmol m^{-2} s^{-1} UV-B. After 21 d, leaves were harvested and measurements were made, as reported above.

To analyze plant survival after stress treatments, plants were grown on plates containing MS (6.5% agar) medium overlaid with a nylon mesh (Prosep) of 20 µM pore size to prevent roots from growing into the medium. After 14 d, plants were transferred to MS medium or MS medium supplemented with either 200 mM mannitol or 150 mM NaCl by gently lifting the nylon mesh with a forceps. After 3 weeks, the percentage of survival was scored. We considered as dead the plants with bleached leaves and as survived the ones with green leaves, then the percentage of survival was calculated by the formula: number of plants survived × 100/total number of plants.

For the UV-B sensitivity assay, 10-day-old plants grown *in vitro* were transferred to soil and, after 3 d, exposed to a supplemental UV-B treatment as reported by Kliebenstein et al. (2002). White light (100 µmol s^{-1} m^{-2}) was supplemented with UV-B from F40 UV-B fluorescent lamps (Philips). Plants were exposed to 5 µmol m^{-2} s^{-1} for 24 h and then returned to white light for 5 d to determine survival.

Generation of Transgenic *Arabidopsis* Plants

UVR8 cDNA was amplified from an *Arabidopsis* cDNA library and cloned into the binary pKYLX71 vector (Schardl et al., 1987) by using the restriction sites *Hind*III and *Xba*I.

The binary constructs were introduced into *Agrobacterium tumefaciens* strain LBA4404 and transformed into *Arabidopsis* Col-0, by the floral dipping method (Bechtold and Pelletier, 1998). Independent transformants were screened on MS medium containing 50 mg L^{-1} kanamycin. The transformed seedlings were transferred to soil after 2–3 weeks. The number of T-DNA insertions was estimated using the ratio of kanamycin-resistant to kanamycin-sensitive plants in the T_2 generation. Homozygous transgenic plants with a single T-DNA insertion were selected from the T_3 generation and used for phenotypic characterization.

DPBA Staining

Individual plants were submerged in an aqueous solution containing 0.01% Triton X-100, 2.52 mg ml^{-1} DPBA, and placed on a rotary shaker at low speed for 7 min. The roots were then washed in de-ionized water for 7 min and mounted between two coverslips. An epifluorescence microscope (Leica) was used to excite the roots at 488 nm. For quantification of DPBA fluorescence, a box was drawn from the elongation zone to the root tip. The average intensity of the fluorescence in this box was recorded by the ImageJ software.

Phenolic Compounds Extraction and Detection

Leaves from *35S-UVR8* and control plants were harvested and lyophilized. One hundred mg of leaves were extracted in 4:46:50 acetic acid:water:methanol, and incubated at 65°C for 30 min, centrifuged at 12 000 *g* for 2 min. Chromatographic analyses were carried out on an 1100 series HPLC (Agilent Technologies) coupled to an Esquire 6000 ESI-Ion Trap mass spectrometer (Bruker Daltonics) operated in alternating ionization mode in the range *m/z* 60–1400. Capillary voltage, –4000 V/4 000 V; nebulizer pressure, 35 psi; drying gas, 11 L min^{-1}; gas temperature, 330°C. Elution was accomplished using a EC 250/4.6 Nucleodur Sphinx RP column (25 cm ×

4.6 mm, 5 µm, Macherey-Nagel) with a gradient of 0.2% (v/v) formic acid (solvent A) and acetonitrile (solvent B) at a flow rate of 1 ml min^{-1} at 25°C as follows: 0%–100% (v/v) B (15 min), 100% B (3 min), 100%–0% (v/v) B (6 s), 0% B (8 min 54 s). Flow coming from the column was diverted in a ratio 4:1 before reaching the ESI unit. Flavonols and sinapoyl derivatives were identified as described by Besseau et al. (2007). Separation and quantification were achieved on a Hewlett Packard HP 1100 Series HPLC system with autosampler and diode-array detector (Agilent Technologies, Böblingen, Germany). A C-18 reversed phase column (Nucleodur Sphinx RP, 250 × 4.6 mm, 5 µm, Macherey-Nagel, Düren, Germany) operated at 1 ml min^{-1} and 25°C and elution was accomplished with a gradient (solvent A 0.2% Formic acid (v:v) solvent B: acetonitrile) of 40% B (15 min), 100% B in 0.10 min (2.5 min hold), 100%–10% B (3.50 min). Quantitative determination was performed on 345-nm absorbance profiles for flavonols and sinapate esthers. Standard curves for apigenin glucoside and sinapic acid were used for quantification of flavonol glycosides and sinapate esthers, respectively.

RNA Extraction, cDNA Synthesis, and qRT–PCR

RNA was extracted from plants grown *in vitro* for 14 d and transferred to MS medium supplemented with 100 mM NaCl or –0.5 MPa PEG, or to starvation conditions (no sugar in the dark) for 24 h, or exposed to UV-B for 2 h, by using the Plant RNeasy mini kit (QIAGEN) according to the manufacturer's instructions. To exclude genomic DNA contamination, 1 µg of RNA was treated with RNase free DNase I (Invitrogen). After DNase digestion, 0.5–1 µg of total RNA was reverse-transcribed with SuperScript II reverse transcriptase (Invitrogen) and oligo-dT primer according to the manufacturer's instructions. qRT–PCR analysis of reverse-transcribed RNA was performed on a Rotor-Gene (QIAGEN/Corbett Research) thermal cycler using SYBR Green master mix (Invitrogen). For the primer design of *UVR8* (5'CCAGATTTCGGGAGGTTGG3' and 5'TTATTGCCGACTCCTACTTGTCC3') and *CHS* (5'TTGTGC ATACATGGCACCTT3' and 5'AAGAGTTTGGGCTGCAGGAGA3'), the software Primer Express™ (Perkin Elmer) was used. Data were analyzed using manufacturer's software by using the *ddct* method (Livak and Schmittgen, 2001). Normalization was done using the genes *18S* (5'CCCAAGGTTCAACTACGAGC3' and 5'TAGATAAAAGGTCGACGCGG3') or *ACT2* (5'AGGAGGTAC AGTGTCTGGATCGG 3'and 5'AACGATTCCTGACCTGCC3').

Protein Extraction, SDS–PAGE, and Western Blot Analysis

To prepare total protein extracts under denaturing conditions, plant material was ground in liquid nitrogen and thawed in extraction buffer containing 100 mM NaH_2PO_4, 10 mM Tris, 4 M urea, and 1 mM PMSF.

For the identification of UVR8 partners, proteins were extracted under native conditions from plants grown *in vitro* under 16-h day/8-h night regime in 110 µmol m^{-2} s^{-1} white light and 0.03 µmol m^{-2} s^{-1} UV-B in the extraction buffer containing 1% NP40, PBS (Sambrook et al., 1989), 1 mM PMSF, and the plant cell protease inhibitor cocktail (Sigma-Aldrich), and the concentration of extracted proteins was determined with the Bio-Rad protein assay. Thirty µg of total protein in sample buffer, containing 100 mM Tris–HCl, pH 6.8, 4% SDS, 0.2% bromphenol blue, 20% glycerol, and 100 mM DTT, was separated on 10% SDS–polyacrylamide gels (Laemmli, 1970) and transferred onto nitrocellulose (Amersham) by electroblotting. Proteins were analyzed by immunoblotting with a polyclonal antibody generated against the 6HIS-UVR8 protein (1:5,000 dilution), as described below. Bound primary antibodies were detected with donkey anti-rabbit, horseradish peroxidase-conjugated secondary antibodies (at 1:10 000 dilution; Amersham) and visualized using reagents for chemiluminescent detection (ECL Plus reagent; Amersham Biosciences).

Recombinant UVR8 Production

The cDNA encoding *UVR8* was amplified by PCR using cDNA from *Arabidopsis* plants. The *Hind*III site and the *Bam*HI site were inserted at the 5' end forward primer and the 3' end reverse primer, respectively, to clone the cDNA in the expression vector pQE31 (Qiagen) containing a 6 His sequence.

The expression of the resulting six His fused proteins was induced with 0.1 mM isopropyl-β-D-thiogalactopyranoside (IPTG) in the *Escherichia coli* M15 strain (Qiagen). Bacterial cells were harvested by centrifugation for 15 min at 5000 *g* at 4°C; cell pellets were re-suspended in sonication buffer (50 mM Tris pH 8.0, 50 mM NaCl, 1 mM EDTA, 0.5 mM PMSF, 0.8% TritonX-100, 0.4% sodium deoxycholate), lysed by sonication, and clarified by centrifugation at 10 000 *g* for 15 min at 4°C. The bacterial pellet was washed with sonication buffer and lysed again by sonication. After centrifugation, the pellet was re-suspended in buffer A (100 mM NaH_2PO_4, 10 mM Tris, 8 M Urea, 5% β-mercaptoethanol) and centrifuged again as described above. The recombinant protein was purified by IMAC affinity chromatography on a HisTrap HP column (GE Healthcare, Chalfont St. Giles, UK), connected to an Akta Purifier system (GE Healthcare), and eluted with buffer C (100 mM NaH_2PO_4, 10 mM Tris pH 7.4, 0.2 M NaCl, 0.5 M imidazole). Collected fractions were analyzed in a 12% SDS–PAGE. The amino acidic sequence of the purified recombinant UVR8 protein was analyzed after trypsin digestion by NanoLC mass spectrometry and the UVR8 peptides were identified by using Mascot against the TAIR protein database.

The purified recombinant UVR8 His-tagged protein was used to raise a polyclonal anti-serum in rabbit (Primm, Milan, Italy).

IAA Quantification

For IAA quantification, samples were treated and analyzed as reported by Hectors et al. (2012). Plant material was ground in a Magna Lyser (5 × 15 s, speed 6500 rpm; Roche Molecular Biochemicals, Mannheim, Germany). IAA and IAA conjugates were extracted overnight in 80% methanol. As internal

standard, 1000 pmol [13C6-phenyl]-IAA (Cambridge Isotope Laboratory Inc., Andover, MA) was added for recovery and quantification by mass spectrometry.

SUPPLEMENTARY DATA

Supplementary Data are available at *Molecular Plant Online*.

FUNDING

This work was supported by the Interuniversity Attraction Poles Programme (IUAP P7/29 'MARS') initiated by the Belgian Science Policy Office, by grants from Ghent University (Bijzonder Onderzoeksfonds Methusalem project no. BOF08/01M00408), and by grants to the MIUR project FIRB Plant-STRESS.

ACKNOWLEDGMENTS

We would like to thank Prof. Jonathan Gershenzon and Michael Reichelt for the help with metabolic analysis, and Lynne Yenoush and Tom Beeckman for theorical and technical assistance. We acknowledge Annick Bleys for help in preparing the manuscript. We also thank the foundation 'Valeria Vincenzo Landi' of Accademia Nazionale dei Lincei for the post-doctoral fellowship awarded to R.F. No conflict of interest declared.

REFERENCES

Achard, P., Cheng, H., De Grauwe, L., Decat, J., Schoutteten, H., Moritz, T., Van Der Straeten, D., Peng, J., and Harberd, N.P. (2006). Integration of plant responses to environmentally activated phytohormonal signals. Science. **311**, 91–94.

Atkinson, N.J., and Urwin, P.E. (2012). The interaction of plant biotic and abiotic stresses: from genes to the field. J. Exp. Bot. **63**, 3523–3543.

Bartels, D., and Sunkar, R. (2005). Drought and salt tolerance in plants. Crit. Rev. Plant Sci. **24**, 23–58.

Bechtold, N., and Pelletier, G. (1998). *In planta Agrobacterium*-mediated transformation of adult *Arabidopsis thaliana* plants by vacuum infiltration. In Arabidopsis Protocols, Martinez-Zapater, J.M., and Salinas, J., eds (Totowa, NJ: Humana Press), pp. 259–266.

Besseau, S., Hoffmann, L., Geoffroy, P., Lapierre, C., Pollet, B., and Legrand, M. (2007). Flavonoid accumulation in *Arabidopsis* repressed in lignin synthesis affects auxin transport and plant growth. Plant Cell. **19**, 148–162.

Bhalerao, R.P., Eklöf, J., Ljung, K., Marchant, A., Bennett, M., and Sandberg, G. (2002). Shoot-derived auxin is essential for early lateral root emergence in *Arabidopsis* seedlings. Plant J. **29**, 325–332.

Boccalandro, H.E., Mazza, C.A., Mazzella, M.A., Casal, J.J., and Ballaré, C.L. (2001). Ultraviolet B radiation enhances a phytochrome-B-mediated photomorphogenic response in *Arabidopsis*. Plant Physiol. **126**, 780–788.

Brown, B.A., and Jenkins, G.I. (2008). UV-B signaling pathways with different fluence-rate response profiles are distinguished in mature *Arabidopsis* leaf tissue by requirement for UVR8, HY5, and HYH. Plant Physiol. **146**, 576–588.

Brown, B.A., Cloix, C., Jiang, G.H., Kaiserli, E., Herzyk, P., Kliebenstein, D.J., and Jenkins, G.I. (2005). A UV-B-specific signaling component orchestrates plant UV protection. Proc. Natl Acad. Sci. U S A. **102**, 18225–18230.

Brown, D.E., Rashotte, A.M., Murphy, A.S., Normanly, J., Tague, B.W., Peer, W.A., Taiz, L., and Muday, G.K. (2001). Flavonoids act as negative regulators of auxin transport *in vivo* in *Arabidopsis*. Plant Physiol. **126**, 524–535.

Buer, C.S., and Djordjevic, M.A. (2009). Architectural phenotypes in the *transparent testa* mutants of *Arabidopsis thaliana*. J. Exp. Bot. **60**, 751–763.

Casimiro, I., Marchant, A., Bhalerao, R.P., Beeckman, T., Dhooge, S., Swarup, R., Graham, N., Inzé, D., Sandberg, G., and Casero, P.J. (2001). Auxin transport promotes *Arabidopsis* lateral root initiation. Plant Cell. **13**, 843–852.

Chaves, M.M., Pereira, J.S., Maroco, J., Rodrigues, M.L., Ricardo, C.P.P., Osório, M.L., Carvalho, I., Faria, T., and Pinheiro, C. (2002). How plants cope with water stress in the field? Photosynthesis and growth. Ann. Bot. **89**, 907–916.

Chen, H., Zhang, J., Neff, M.M., Hong, S.-W., Zhang, H., Deng, X.-W., and Xiong, L. (2008). Integration of light and abscisic acid signaling during seed germination and early seedling development. Proc. Natl Acad. Sci. U S A. **105**, 4495–4500.

Chen, M., Chory, J., and Fankhauser, C. (2004). Light signal transduction in higher plants. Annu. Rev. Genet. **38**, 87–117.

Christie, J.M., Arvai, A.S., Baxter, K.J., Heilmann, M., Pratt, A.J., O'Hara, A., Kelly, S.M., Hothorn, M., Smith, B.O., and Hitomi, K. (2012). Plant UVR8 photoreceptor senses UV-B by tryptophan-mediated disruption of cross-dimer salt bridges. Science. **335**, 1492–1496.

Claeys, H., and Inzé, D. (2013). The agony of choice: how plants balance growth and survival under water-limiting conditions. Plant Physiol., **162**, 1768–1779.

Cloix, C., Kaiserli, E., Heilmann, M., Baxter, K.J., Brown, B.A., O'Hara, A., Smith, B.O., Christie, J.M., and Jenkins, G.I. (2012). C-terminal region of the UV-B photoreceptor UVR8 initiates signaling through interaction with the COP1 protein. Proc. Natl Acad. Sci. U S A. **109**, 16366–16370.

Comont, D., Winters, A., and Gwynn-Jones, D. (2012). Acclimation and interaction between drought and elevated UV-B in *A. thaliana:* differences in response over treatment, recovery and reproduction. Ecol. Evol. **2**, 2695–2709.

Cramer, G.R., Urano, K., Delrot, S., Pezzotti, M., and Shinozaki, K. (2011). Effects of abiotic stress on plants: a systems biology perspective. BMC Plant Biol. **11**, 163.

De Smet, I., and Jürgens, G. (2007). Patterning the axis in plants-auxin in control. Curr. Opin. Genet. Dev. **17**, 337–343.

Dubrovsky, J.G., and Forde, B.G. (2012). Quantitative analysis of lateral root development: pitfalls and how to avoid them. Plant Cell. **24**, 4–14.

Dubrovsky, J.G., Napsucialy-Mendivil, S., Duclercq, J., Cheng, Y., Shishkova, S., Ivanchenko, M.G., Friml, J., Murphy, A.S., and Benková, E. (2011). Auxin minimum defines a developmental window for lateral root initiation. New Phytol. **191**, 970–983.

Farooq, M., Wahid, A., Kobayashi, N., Fujita, D., and Basra, S.M.A. (2009). Plant drought stress: effects, mechanisms and management. Agron. Sustain. Dev. **29**, 185–212.

Favory, J.-J., Stec, A., Gruber, H., Rizzini, L., Oravecz, A., Funk, M., Albert, A., Cloix, C., Jenkins, G.I., and Oakeley, E.J. (2009). Interaction of COP1 and UVR8 regulates UV-B-induced photomorphogenesis and stress acclimation in *Arabidopsis*. EMBO J. **28**, 591–601.

Frohnmeyer, H., and Staiger, D. (2003). Ultraviolet-B radiation-mediated responses in plants: balancing damage and protection. Plant Physiol. **133**, 1420–1428.

Fukai, S., and Cooper, M. (1995). Development of drought-resistant cultivars using physiomorphological traits in rice. Field Crop. Res. **40**, 67–86.

Gitz, D.C., and Liu-Gitz, L. (2003). How do UV photomorphogenic responses confer water stress tolerance? Photochem. Photobiol. **78**, 529–534.

Gonzalez, N., De Bodt, S., Sulpice, R., Jikumaru, Y., Chae, E., Dhondt, S., Van Daele, T., De Milde, L., Weigel, D. and Kamiya, Y. (2010). Increased leaf size: different means to an end. Plant Physiol. **153**, 1261–1279.

Grunewald, W., De Smet, I., Lewis, D.R., Löfke, C., Jansen, L., Goeminne, G., Vanden Bossche, R., Karimi, M., De Rybel, B. and Vanholme, B. (2012). Transcription factor WRKY23 assists auxin distribution patterns during *Arabidopsis* root development through local control on flavonol biosynthesis. Proc. Natl Acad. Sci. U S A. **109**, 1554–1559.

Guo, P., Baum, M., Grando, S., Ceccarelli, S., Bai, G., Li, R., von Korff, M., Varshney, R.K., Graner, A., and Valkoun, J. (2009). Differentially expressed genes between drought-tolerant and drought-sensitive barley genotypes in response to drought stress during the reproductive stage. J. Exp. Bot. **60**, 3531–3544.

Hectors, K., Jacques, E., Prinsen, E., Guisez, Y., Verbelen, J.-P., Jansen, M.A.K., and Vissenberg, K. (2010). UV radiation reduces epidermal cell expansion in leaves of *Arabidopsis thaliana*. J. Exp. Bot. **61**, 4339–4349.

Hectors, K., van Oevelen, S., Guisez, Y., Prinsen, E., and Jansen, M.A.K. (2012). The phytohormone auxin is a component of the regulatory system that controls UV-mediated accumulation of flavonoids and UV-induced morphogenesis. Physiol. Plant. **145**, 594–603.

Heuer, B., and Nadler, A. (1995). Growth and development of potatoes under salinity and water deficit. Aust. J. Agric. Res. **46**, 1477–1486.

Hruz, T., Laule, O., Szabo, G., Wessendorp, F., Bleuler, S., Oertle, L., Widmayer, P., Gruissem, W., and Zimmermann, P. (2008). Genevestigator V3: a reference expression database for the meta-analysis of transcriptomes. Adv. Bioinformatics. **2008**, 420747.

Hughes, N.M., Reinhardt, K., Feild, T.S., Gerardi, A.R., and Smith, W.K. (2010). Association between winter anthocyanin production and drought stress in angiosperm evergreen species. J. Exp. Bot. **61**, 1699–1709.

Ito, H., Fukuda, Y., Murata, K., and Kimura, A. (1983). Transformation of intact yeast cells treated with alkali cations. J. Bacteriol. **153**, 163–168.

Jaleel, C.A., Manivannan, P., Wahid, A., Farooq, M., Al-Juburi, H.J., Somasundaram, R., and Panneerselvam, R. (2009). Drought stress in plants: a review on morphological characteristics and pigments composition. International Journal of Agriculture and Biology. **11**, 100–105.

Jansen, M.A.K. (2002). Ultraviolet-B radiation effects on plants: induction of morphogenic responses. Physiol. Plant. **116**, 423–429.

Jenkins, G.I. (2009). Signal transduction in responses to UV-B radiation. Annu. Rev. Plant Biol. **60**, 407–431.

Jiang, L., Wang, Y., Björn, L.O., and Li, S. (2009). *Arabidopsis RADICAL-INDUCED CELL DEATH1 is* involved in UV-B signaling. Photochem. Photobiol. Sci. **8**, 838–846.

Jiang, L., Wang, Y., Li, Q.-F., Björn, L.O., He, J.-X., and Li, S.-S. (2012). *Arabidopsis* STO/BBX24 negatively regulates UV-B signaling by interacting with COP1 and repressing HY5 transcriptional activity. Cell Res. **22**, 1046–1057.

Katiyar-Agarwal, S., Zhu, J., Kim, K., Agarwal, M., Fu, X., Huang, A., and Zhu, J.-K. (2006). The plasma membrane Na^+/H^+ antiporter SOS1 interacts with RCD1 and functions in oxidative stress tolerance in *Arabidopsis*. Proc. Natl Acad. Sci. U S A. **103**, 18816–18821.

Kim, B.C., Tennessen, D.J., and Last, R.L. (1998). UV-B-induced photomorphogenesis in *Arabidopsis thaliana.* Plant J. **15**, 667–674.

Kliebenstein, D.J., Lim, J.E., Landry, L.G., and Last, R.L. (2002). *Arabidopsis UVR8* regulates ultraviolet-B signal transduction and tolerance and contains sequence similarity to human *regulator of chromatin condensation 1*. Plant Physiol. **130**, 234–243.

Laemmli, U.K. (1970). Cleavage of structural proteins during the assembly of the head of bacteriophage T4. Nature. **227**, 680–685.

Lee, K.S., Hines, L.K., and Levin, D.E. (1993). A pair of functionally redundant yeast genes (PPZ1 and PPZ2) encoding type 1-related protein phosphatases function within the PKC1-mediated pathway. Mol. Cell. Biol. **13**, 5843–5853.

Liao, H., Rubio, G., Yan, X., Cao, A., Brown, K.M., and Lynch, J.P. (2001). Effect of phosphorus availability on basal root shallowness in common bean. Plant Soil. **232**, 69–79.

Lippuner, V., Cyert, M.S., and Gasser, C.S. (1996). Two classes of plant cDNA clones differentially complement yeast calcineurin mutants and increase salt tolerance of wild-type yeast. J. Biol. Chem. **271**, 12859–12866.

Livak, K.J., and Schmittgen, T.D. (2001). Analysis of relative gene expression data using real-time quantitative PCR and the $2^{-\Delta\Delta CT}$ method. Methods. **25**, 402–408.

Malamy, J.E., and Benfey, P.N. (1997). Organization and cell differentiation in lateral roots of *Arabidopsis thaliana*. Development. **124**, 33–44.

Merchan, S., Bernal, D., Serrano, R., and Yenush, L. (2004). Response of the *Saccharomyces cerevisiae* Mpk1 mitogen-activated protein kinase pathway to increases in internal turgor pressure caused by loss of Ppz protein phosphatases. Eukaryot. Cell. **3**, 100–107.

Minet, M., Dufour, M.-E., and Lacroute, F. (1992). Cloning and sequencing of a human cDNA coding for dihydroorotate dehydrogenase by complementation of the corresponding yeast mutant. Gene. **121**, 393–396.

Morales, L.O., Brosché, M., Vainonen, J., Jenkins, G.I., Wargent, J.J., Sipari, N., Strid, Å., Lindfors, A.V., Tegelberg, R., and Aphalo, P.J. (2012). Multiple roles for UV RESISTANCE LOCUS 8 in regulating gene expression and metabolite accumulation in *Arabidopsis* under solar UV radiation. Plant Physiol., 18 December, 10.1104/pp.112.211375.

Murashige, T., and Skoog, F. (1962). A revised medium for rapid growth and bio assays with tobacco tissue cultures. Physiol. Plant. **15**, 473–497.

O'Hara, A., and Jenkins, G.I. (2013). *In vivo* function of tryptophans in the *Arabidopsis* UV-B photoreceptor UVR8. Plant Cell. **24**, 3755–3766.

Oravecz, A., Baumann, A., Máté, Z., Brzezinska, A., Molinier, J., Oakeley, E.J., Ádám, E., Schäfer, E., Nagy, F., and Ulm, R. (2006). CONSTITUTIVELY PHOTOMORPHOGENIC1 is required for the UV-B response in *Arabidopsis*. Plant Cell. **18**, 1975–1990.

Osterlund, M.T., Hardtke, C.S., Wei, N., and Deng, X.W. (2000). Targeted destabilization of HY5 during light-regulated development of *Arabidopsis*. Nature. **405**, 462–466.

Pardo, J.M. (2010). Biotechnology of water and salinity stress tolerance. Curr. Opin. Biotechnol. **21**, 185–196.

Park, C.-M. (2007). Auxin homeostasis in plant stress adaptation response. Plant Signal. Behav. **2**, 306–307.

Park, J.-E., Park, J.-Y., Kim, Y.-S., Staswick, P.E., Jeon, J., Yun, J., Kim, S.-Y., Kim, J., Lee, Y.-H., and Park, C.-M. (2007). GH3-mediated auxin homeostasis links growth regulation with stress adaptation response in *Arabidopsis*. J. Biol. Chem. **282**, 10036–10046.

Peer, W.A., and Murphy, A.S. (2007). Flavonoids and auxin transport: modulators or regulators? Trends Plant Sci. **12**, 556–563.

Potters, G., Pasternak, T.P., Guisez, Y., and Jansen, M.A.K. (2009). Different stresses, similar morphogenic responses: integrating a plethora of pathways. Plant Cell and Environment. **32**, 158–169.

Potters, G., Pasternak, T.P., Guisez, Y., Palme, K.J., and Jansen, M.A.K. (2007). Stress-induced morphogenic responses: growing out of trouble? Trends Plant Sci. **12**, 98–105.

Poulson, M.E., Boeger, M.R.T., and Donahue, R.A. (2006). Response of photosynthesis to high light and drought for *Arabidopsis thaliana* grown under a UV-B enhanced light regime. Photosynth. Res. **90**, 79–90.

Price, A.H., Tomos, A.D., and Virk, D.S. (1997). Genetic dissection of root growth in rice (*Oryza sativa* L.) I: a hydrophonic screen. Theor. Appl. Genet. **95**, 132–142.

Rizzini, L., Favory, J.-J., Cloix, C., Faggionato, D., O'Hara, A., Kaiserli, E., Baumeister, R., Schäfer, E., Nagy, F. and Jenkins, G.I. (2011). Perception of UV-B by the *Arabidopsis* UVR8 Protein. Science. **332**, 103–106.

Saijo, Y., Sullivan, J.A., Wang, H., Yang, J., Shen, Y., Rubio, V., Ma, L., Hoecker, U., and Deng, X.W. (2003). The COP1–SPA1 interaction defines a critical step in phytochrome A-mediated regulation of HY5 activity. Genes Dev. **17**, 2642–2647.

Sambrook, J., Fritch, E.F., and Maniatis, T. (1989). Molecular Cloning: A Laboratory Manual (Cold Spring Harbor, NY: Cold Spring Harbor Laboratory Press).

Schardl, C.L., Byrd, A.D., Benzion, G., Altschuler, M.A., Hildebrand, D.F., and Hunt, A.G. (1987). Design and construction of a versatile system for the expression of foreign genes in plants. Gene. **61**, 1–11.

Sharp, R.E., Poroyko, V., Hejlek, L.G., Spollen, W.G., Springer, G.K., Bohnert, H.J., and Nguyen, H.T. (2004). Root growth maintenance during water deficits: physiology to functional genomics. J. Exp. Bot. **55**, 2343–2351.

Sibout, R., Sukumar, P., Hettiarachchi, C., Holm, M., Muday, G.K., and Hardtke, C.S. (2006). Opposite root growth phenotypes of *hy5* versus *hy5 hyh* mutants correlate with increased constitutive auxin signaling. PLoS Genet. **2**, e202.

Skirycz, A., and Inzé, D. (2010). More from less: plant growth under limited water. Curr. Opin. Biotechnol. **21**, 197–203.

Skirycz, A., De Bodt, S., Obata, T., De Clercq, I., Claeys, H., De Rycke, R., Andriankaja, M., Van Aken, O., Van Breusegem, F. and Fernie, A.R. (2010). Developmental stage specificity and the role of mitochondrial metabolism in the response of *Arabidopsis* leaves to prolonged mild osmotic stress. Plant Physiol. **152**, 226–244.

Specht, J.E., Chase, K., Macrander, M., Graef, G.L., Chung, J., Markwell, J.P., Germann, M., Orf, J.H., and Lark, K.G. (2001). Soybean response to water: a QTL analysis of drought tolerance. Crop Sci. **41**, 493–509.

Suesslin, C., and Frohnmeyer, H. (2003). An *Arabidopsis* mutant defective in UV-B light-mediated responses. Plant J. **33**, 591–601.

Taylor, L.P., and Grotewold, E. (2005). Flavonoids as developmental regulators. Curr. Opin. Plant Biol. **8**, 317–323.

Tohge, T., Kusano, M., Fukushima, A., Saito, K., and Fernie, A.R. (2011). Transcriptional and metabolic programs following exposure of plants to UV-B irradiation. Plant Signal. Behav. **6**, 1987–1992.

Ulm, R., and Nagy, F. (2005). Signalling and gene regulation in response to ultraviolet light. Curr. Opin. Plant Biol. **8**, 477–482.

Ulm, R., Baumann, A., Oravecz, A., Máté, Z., Ádám, E., Oakeley, E.J., Schäfer, E., and Nagy, F. (2004). Genome-wide analysis of gene expression reveals function of the bZIP transcription factor HY5 in the UV-B response of *Arabidopsis*. Proc. Natl Acad. Sci. U S A. **101**, 1397–1402.

Verslues, P.E., Agarwal, M., Katiyar-Agarwal, S., Zhu, J., and Zhu, J.-K. (2006). Methods and concepts in quantifying resistance to drought, salt and freezing, abiotic stresses that affect plant water status. Plant J. **45**, 523–539.

Wargent, J.J., Gegas, V.C., Jenkins, G.I., Doonan, J.H., and Paul, N.D. (2009a). UVR8 in *Arabidopsis thaliana* regulates multiple aspects of cellular differentiation during leaf development in response to ultraviolet B radiation. New Phytol. **183**, 315–326.

Wargent, J.J., Moore, J.P., Ennos, A.R., and Paul, N.D. (2009b). Ultraviolet radiation as a limiting factor in leaf expansion and development. Photochem. Photobiol. **85**, 279–286.

Werner, T., Nehnevajova, E., Köllmer, I., Novák, O., Strnad, M., Krämer, U., and Schmülling, T. (2010). Root-specific reduction of cytokinin causes enhanced root growth, drought tolerance, and leaf mineral enrichment in *Arabidopsis* and tobacco. Plant Cell. **22**, 3905–3920.

Winter, D., Vinegar, B., Nahal, H., Ammar, R., Wilson, G.V., and Provart, N.J. (2007). An 'electronic fluorescent pictograph' browser for exploring and analyzing large-scale biological data sets. PLoS One. **2**, e718.

Wu, D., Hu, Q., Yan, Z., Chen, W., Yan, C., Huang, X., Zhang, J., Yang, P., Deng, H. and Wang, J. (2012). Structural basis of ultraviolet-B perception by UVR8. Nature. **484**, U214–U296.

Wu, Q.-S., Xia, R.-X., and Zou, Y.-N. (2008). Improved soil structure and citrus growth after inoculation with three arbuscular mycorrhizal fungi under drought stress. Eur. J. Soil Biol. **44**, 122–128.

Xiong, L., and Zhu, J.-K. (2002). Salt tolerance. Arabidopsis Book. **1**, e0048.

Zhang, S.-W., Li, C.-H., Cao, J., Zhang, Y.-C., Zhang, S.-Q., Xia, Y.-F., Sun, D.-Y., and Sun, Y. (2009). Altered architecture and enhanced drought tolerance in rice via the down-regulation of indole-3-acetic acid by *TLD1/OsGH3.13* activation. Plant Physiol. **151**, 1889–1901.

Zhao, Y. (2010). Auxin biosynthesis and its role in plant development. Annu. Rev. Plant Biol. **61**, 49–64.

SUMMARY

This work is focused on the role of the *UVR8* gene in the general reduction of plant growth under osmotic stress and low levels of UV-B light through the inhibition of cell expansion, the *UVR8*-mediated accumulation of flavonoid, and possibly changes in auxin homeostasis.

SUPPLEMENTAL DATA

Supplemental Table 1. Expression values for *UVR8* gene under abiotic stresses from Arabidopsis eFP Browser

Tissue	Sample signal	Control signal	Log2 Ratio	Fold-Change	Links
Control Shoot After 24 Hours	141.69	141.69	0.0	1.0	To the Experiment
Cold Shoot After 24 Hours	228.82	141.69	0.69	1.61	To the Experiment
Osmotic Shoot After 24 Hours	312.88	141.69	1.14	**2.2**	To the Experiment
Salt Shoot After 24 Hours	206.87	141.69	0.54	**1.46**	To the Experiment
Drought Shoot After 24 Hours	184.13	141.69	0.37	1.29	To the Experiment
Genotoxic Shoot After 24 Hours	161.22	141.69	0.18	1.13	To the Experiment
Oxidative Shoot After 24 Hours	163.95	141.69	0.21	1.15	To the Experiment
UV-B Shoot After 24 Hours	133.04	141.69	-0.1	0.93	To the Experiment
Wounding Shoot After 24 Hours	92.18	141.69	-0.63	0.65	To the Experiment
Heat Shoot After 24 Hours	80.59	141.69	-0.82	0.56	To the Experiment
Control Root After 24 Hours	128.43	128.43	0.0	1.0	To the Experiment
Cold Root After 24 Hours	101.24	128.43	-0.35	0.78	To the Experiment
Osmotic Root After 24 Hours	134.37	128.43	0.06	1.04	To the Experiment
Salt Root After 24 Hours	92.21	128.43	-0.48	0.71	To the Experiment
Drought Root After 24 Hours	148.33	128.43	0.2	1.15	To the Experiment
Genotoxic Root After 24 Hours	145.22	128.43	0.17	1.13	To the Experiment
Oxidative Root After 24 Hours	133.71	128.43	0.05	1.04	To the Experiment
UV-B Root After 24 Hours	165.31	128.43	0.36	1.28	To the Experiment
Wounding Root After 24 Hours	128.11	128.43	-0.01	0.99	To the Experiment
Heat Root After 24 Hours	59.21	128.43	-1.12	0.46	To the Experiment

Supplemental Table 2. Expression values for *UVR8* gene under abiotic stresses from Genevestigator

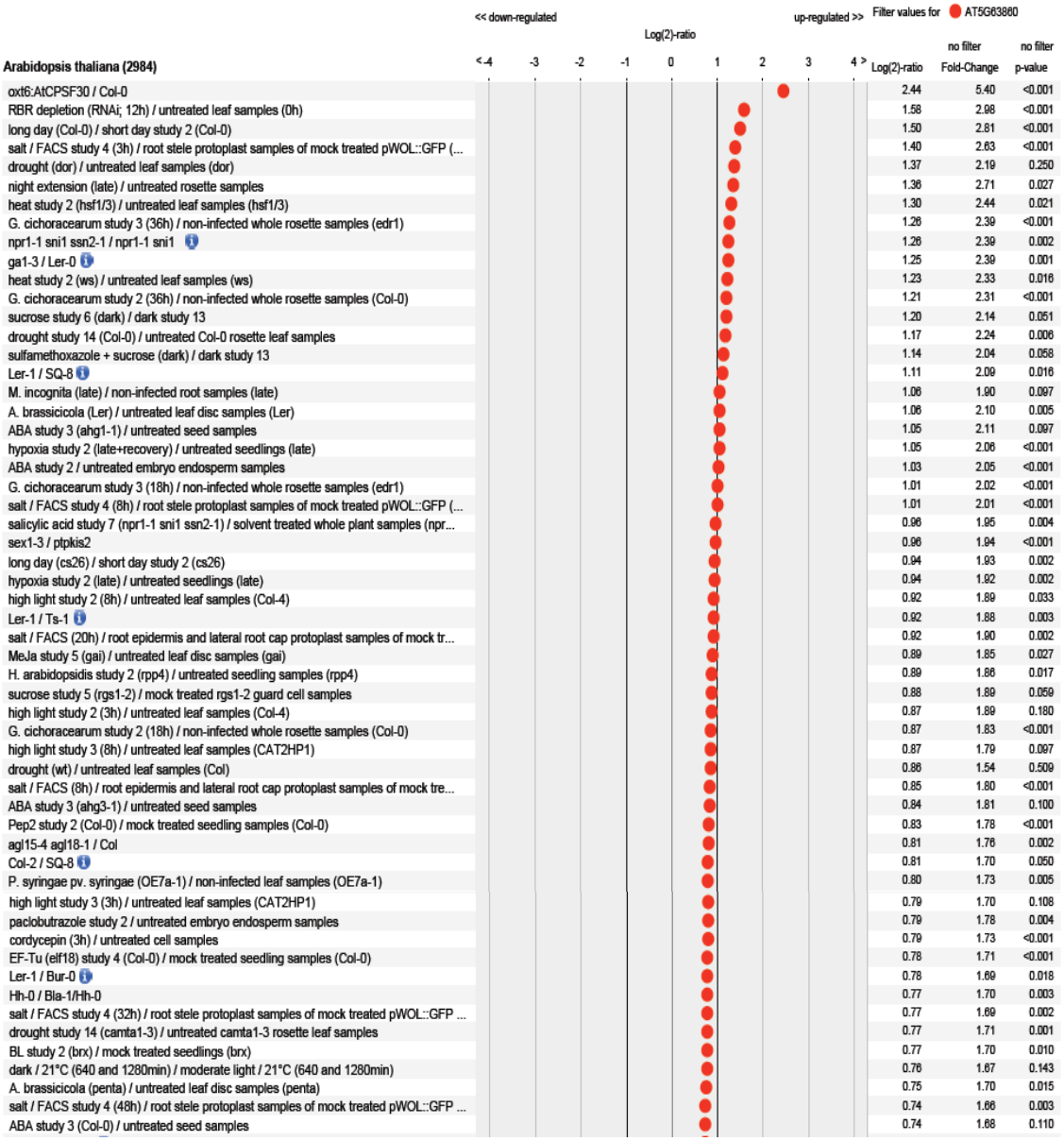

Supplemental Table 3. *Morphological comparison among wild type and uvr8-6 plants*

Parameter	**Wild type**	***uvr8-6***
shoot		
Cotyledon size (mm^2)[a]	3.0 ± 0.1	3.4 ± 0.07*
Hypocotyl length (mm)[a]	1.2 ± 0.04	1.2 ± 0.03
Petiol length (mm)[a]	1.03 ± 0.04	1.15 ± 0.02*
root		
Primary root length (mm)[a]	21.0 ± 0.53	21.14 ± 0.42
Cortex cells (No.)[a]	n.d.	n.d.
Total Primordia (No.)[a]	153 (n=14)	151 (n=14)
Primary root length (mm)[b]	27.7± 0.92	30.1 ± 0.74
Lateral root density (No. /cm)[b]	0.28 ± 0.01	0.26 ± 0.01
Lateral root length (cm)[b]	n.d.	n.d.

The bold case indicates the age of the plants used for the measurements. **a** 7 days old seedlings grown *in vitro* on MS plates supplemented with 1% sucrose (shoot) or 1.5% sucrose (root) in a growth chamber at 23^0C under continuous light. **b** 10 days old seedlings. At least 25 plants were used for the analysis. Data shown are averages ± SE. *$P < 0.05$.

Supplemental Table 4. *Morphological comparison among root of wild type and uvr8-6 plants*

Parameter	**Control**	**uvr8-6**
Primary root length (mm)[a]	22.3 ± 3.2	22.2 ± 2.3
Cortex cells (No.)[a]	n.d.	n.d.
Total Primordia (No.)[a]	130	128
Primary root length (cm)[b]	6.5 ± 0.8	6.2 ± 0.83
Lateral root density (No. /cm)[b]	2.1 ± 0.37	2 .0 ± 0.4
Lateral root length (cm)[b]	2 ± 0.77	1.8 ± 0.4

The bold case indicates the age of the plants used for the measurements. **a** 7 days old seedlings grown *in vitro* in a growth chamber at 23^0C under a 16-h-light/8-h-dark photoperiod. **b** 14 days old seedlings. At least 25 plants were used for the analysis. Data shown are averages ± SE.

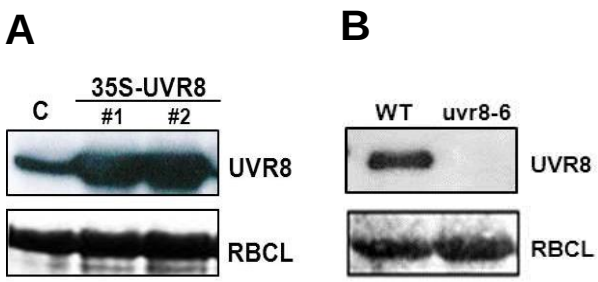

Supplemental Figure 1 Levels of UVR8 protein in *Arabidopis* transgenic plants used in this study. **(A)** UVR8 accumulation in two independent *UVR8* overexpressing lines in comparison to the control plants (C) transformed with empty vector. **(B)** UVR8 levels in the uvr8-6 mutant compared to the wild type plants (WT). Western blotting analysis was performed with an anti-UVR8 antibody. Rubisco large subunity (RBCL) was used as loading control by Ponceau staining of the membrane.

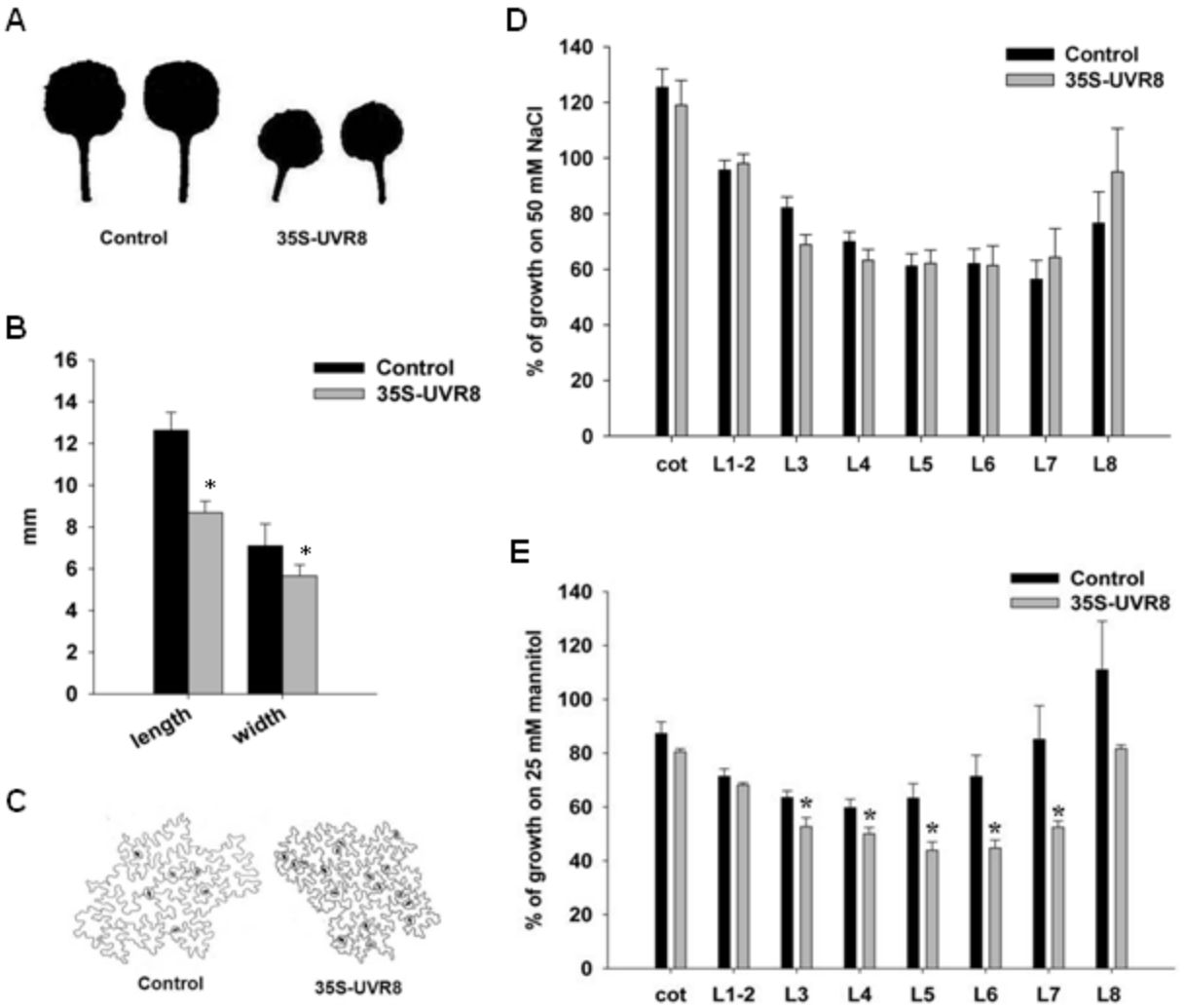

Supplemental Figure 2 (A) Representative leaf 1 and 2 from Control and *35S-UVR8* plants. **(B)** Length and width measurement of the leaves 1 and 2. Values are averages ± SD (n = 14; * P , 0.05). **(C)** Adaxial epidermal cells from the upper region of the leaves 1 and 2 from Control and *35S-UVR8* plants. **(D)** Leaf measurements of Control and *35S-UVR8* plants grown on MS NaCl (50 mM) or mannitol (25 mM) **(E)**. Plants were grown for 21 days on MS supplemented with NaCl or mannitol, then the area of individual leaves was measured. The percentage of growth was calculated as the ratio between the area of the leaves from plants grown on mild stress and that one from plants of the same genotype grown on MS and compared to that one of the Control plants. Data are averages of two independent experiments ± SE (n = 14; * P, 0.05).

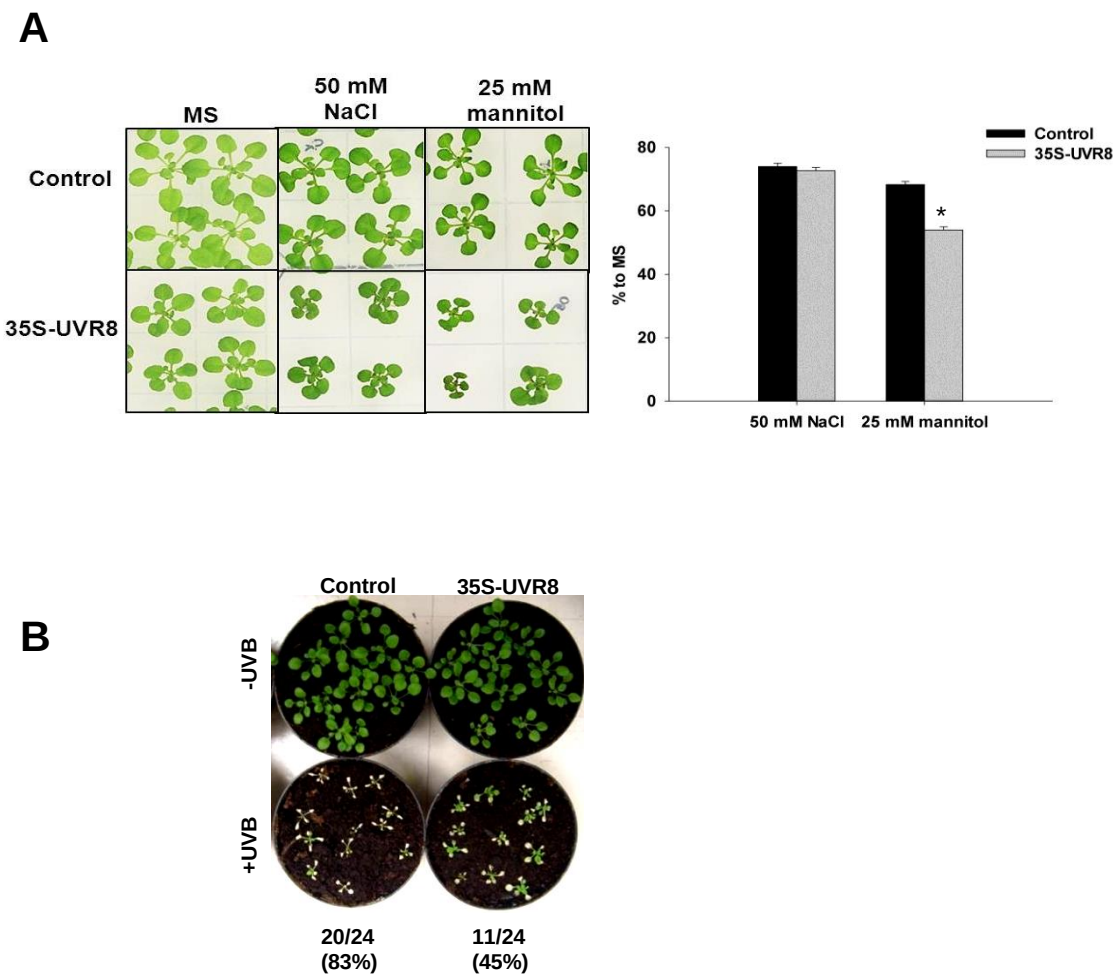

Supplemental Figure 3 (A) Growth analysis on mild stress conditions. Plants were grown for 21 days on MS supplemented with NaCl (50 mM) or mannitol (25 mM) and on MS media used as control, then the area of individual leaves was measured. The percentage difference of rosette size was calculated as the ratio between the rosette area of plants grown on mild stress and on MS. Data are averages ± SE (n = 14; *, P = 0.05).

(B) Twelve-day-old *35S-UVR8* or control plants were exposed to UV-B light for 24 h (+UV-B) or grown under mylar filter used to screen out UV-B light (-UV-B). Plants were photographed after return to white light for 5 days and the percentage of dead plants was recorded.

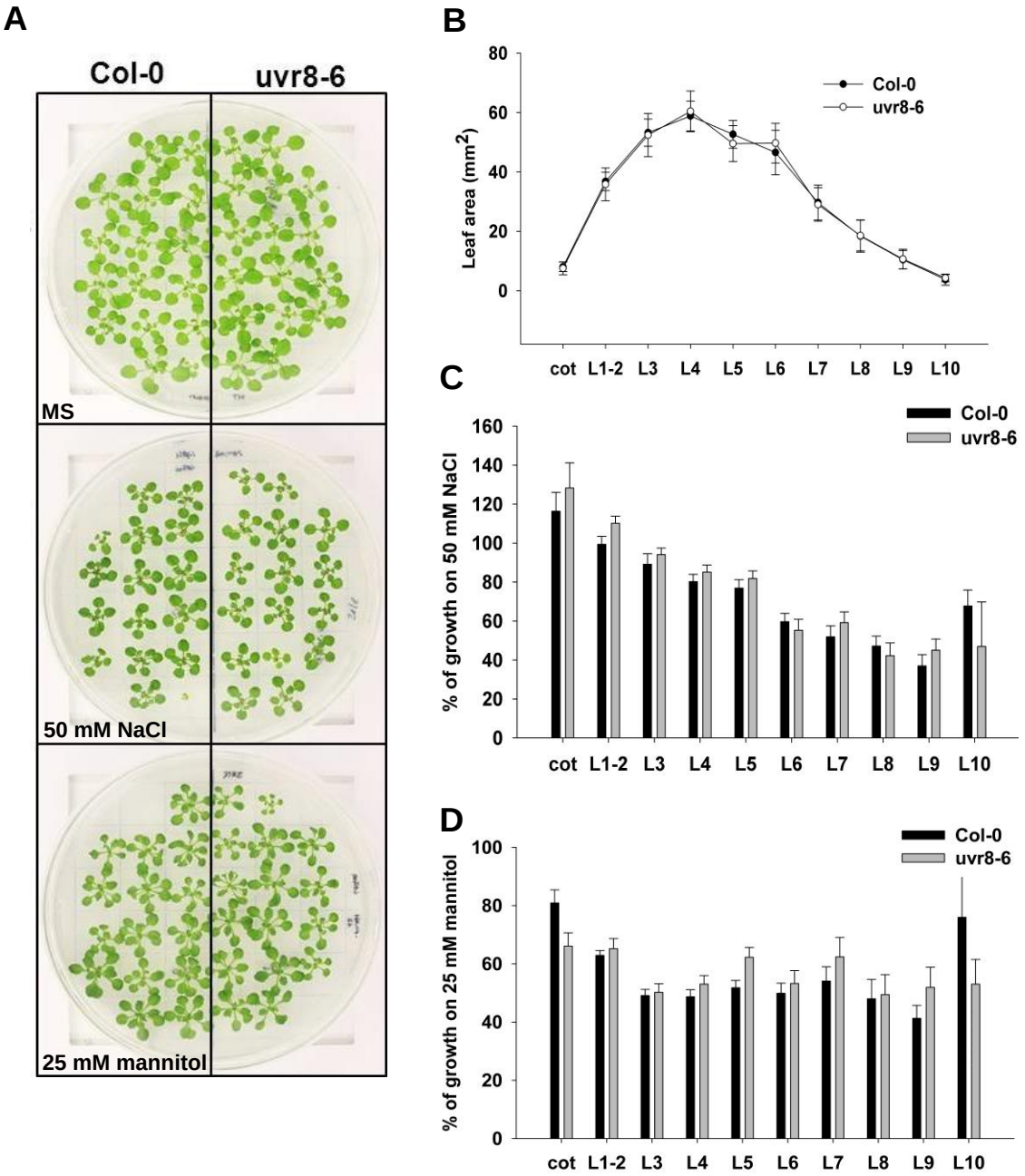

Supplemental Figure 4 (A) Phenotypes of *uvr8-6* plants grown for 21 days on MS or on MS supplemented with NaCl (50 mM) or mannitol (25 mM) respectively. **(B)** Area of rosette leaves at different positions harvested from *uvr8-6* plants grown for 21 days on MS. Values are averages ± SD (n = 14; * P , 0.05). **(C-D)** Response of *uvr8-6* plants to mild stress. Plants were grown for 21 days on MS supplemented with NaCl (50 mM) or mannitol (25 mM) respectively, and on MS media used as control, then the area of individual leaves was measured. The percentage of growth of *uvr8-6* plants on 50 mM NaCl or 25 mM mannitol was calculated as the ratio between the area of the leaves from plants grown on mild stress and that one from plants of the same genotype grown on MS and compared to that one of the control plants. Data are averages of two independent experiments ± SE (n = 14; * P , 0.05)

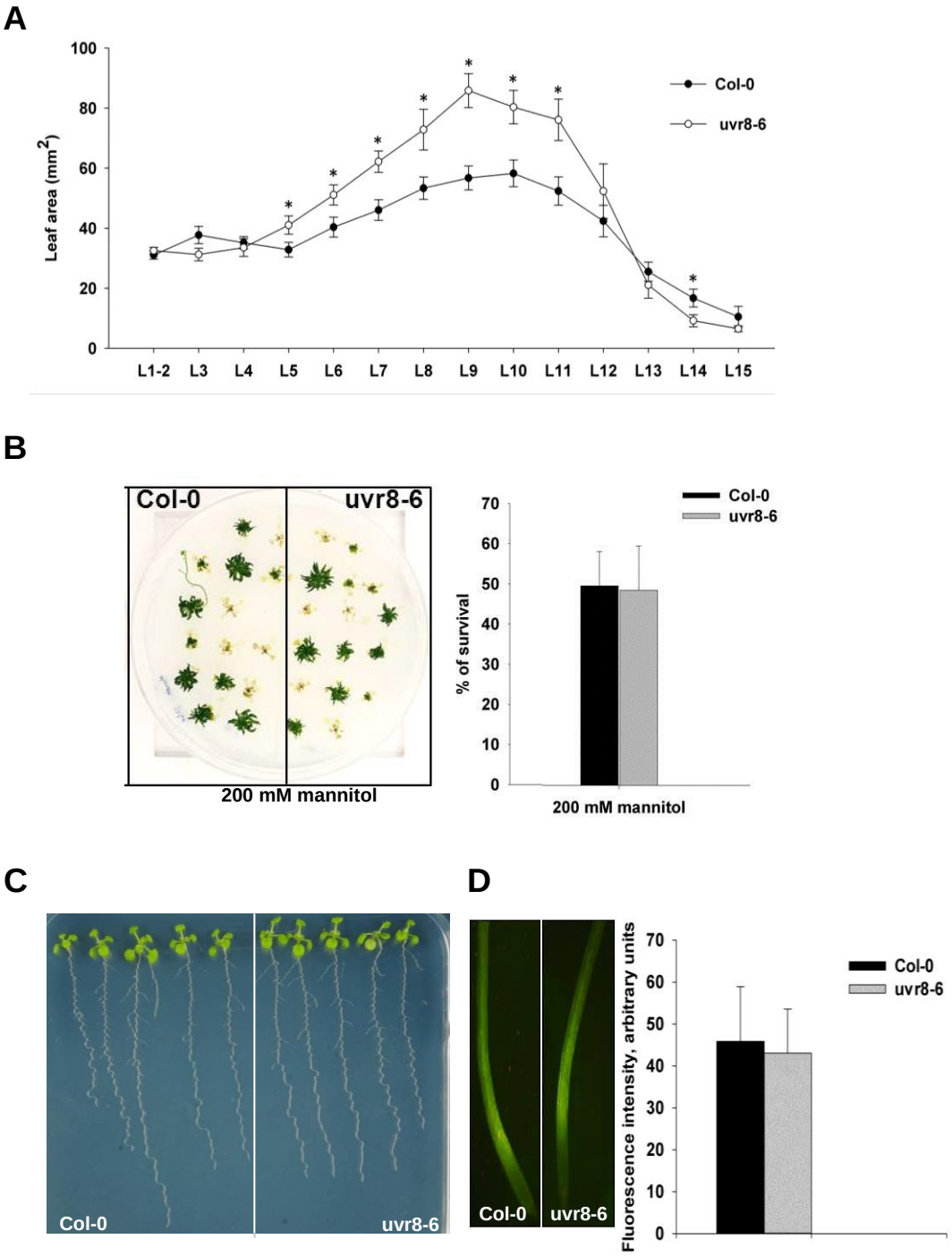

Supplemental Figure 5 (A) Area of rosette leaves at different positions harvested from *uvr8-6* plants grown for three weeks on 150 mM NaCl. Values are averages ± SD (n = 14; *, P = 0.05). **(B)** Growth analysis on severe stress conditions. Plants were grown *in vitro* for 2 weeks on meshes placed on MS medium and transferred on MS media supplemented with mannitol (200 mM). Plants were photographed after three weeks and the percentage of survival was recorded. The results are averages of two independent replicates (n = 70-80) ± SD. **(C)** Root phenotypes of *uvr8-6* mutant plants 14-days old grown *in vitro* in a growth chamber at 23^0C under a 16-h-light/8-h-dark photoperiod. **(D)** DPBA-visualized flavonol accumulation in *uvr8-6* 7-day-old seedlings compared to the control plants and intensity of fluorescence calculated by Image J. Data are averages ± SE (n=12-16)

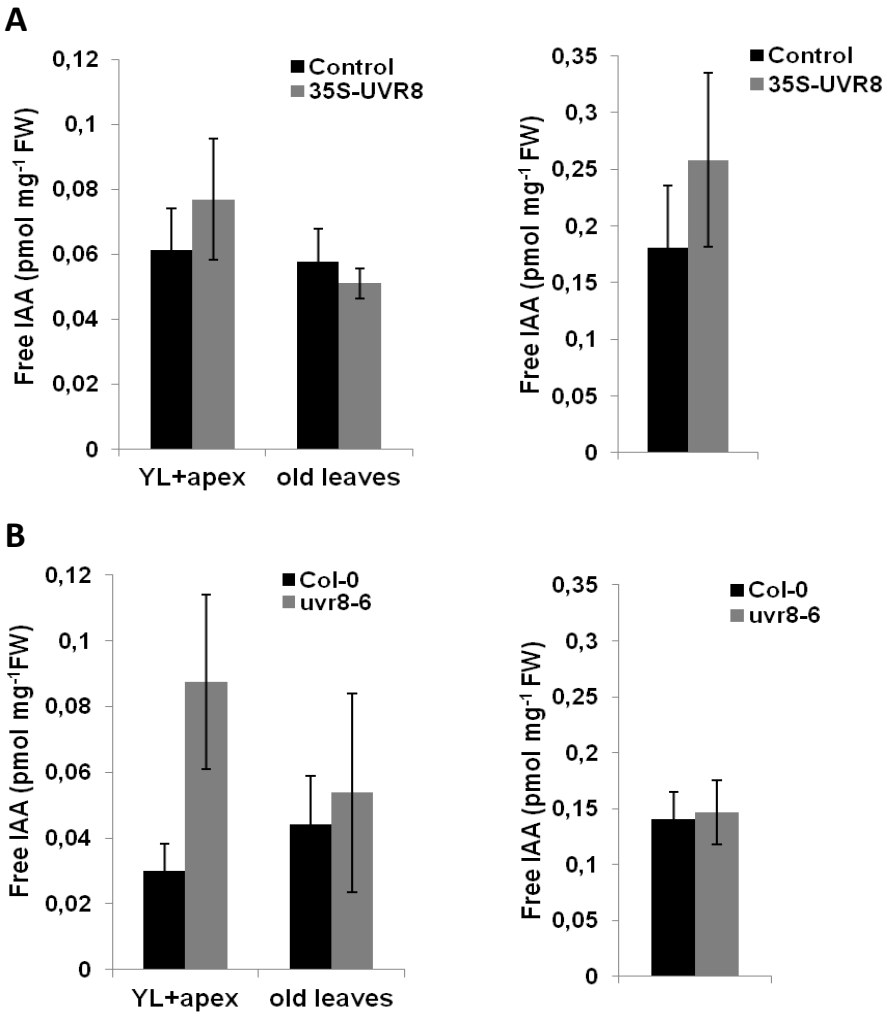

Supplemental Figure 6 Free IAA measurements. (A) Free IAA conjugates in leaves (on the left; YL= young leaves) or roots (on the right) of *35S-UVR8* plants compared to the control. (B) Free IAA conjugates in *uvr8-6* mutant plants. IAA was extracted from young leaves (1-6) and old leaves (7-10) of plants 21 days old grown *in vitro* in a growth chamber at 23^0C under a 16-h-light/8-h-dark photoperiod or from roots of seedling 7 days old grown under continuous light. Values are averages ± SD (n = 3)

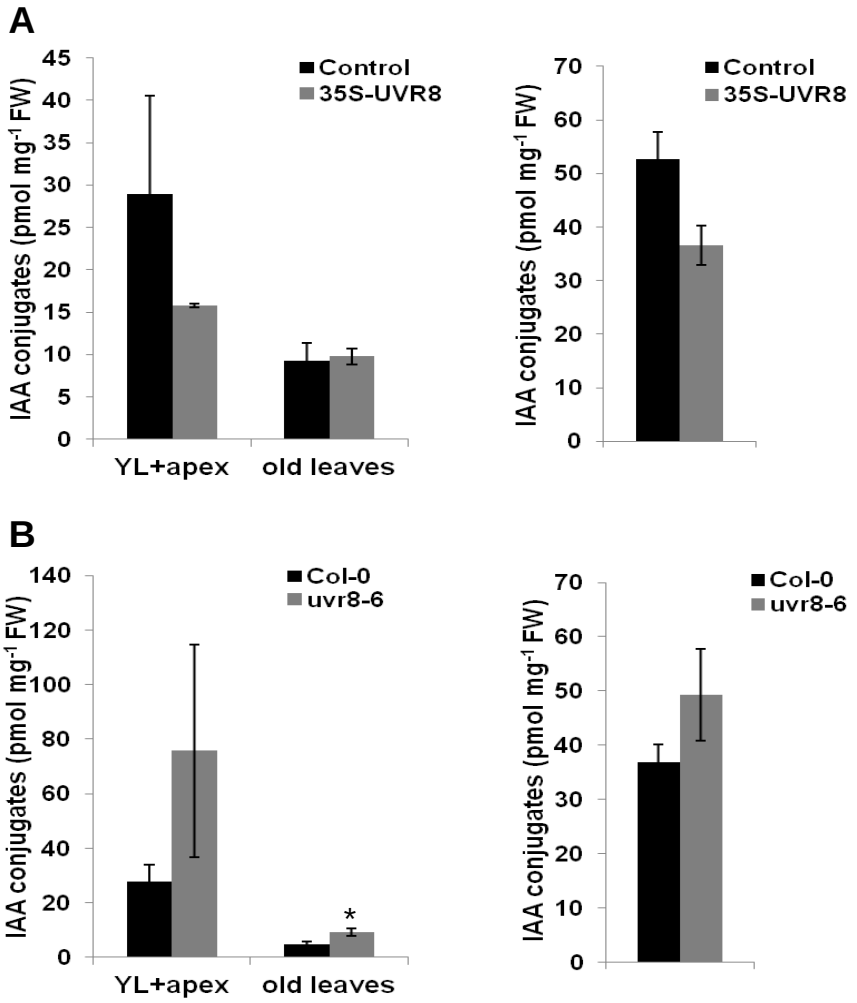

Supplemental Figure 7 IAA Conjugates Measurements.
(A) IAA conjugates in leaves (on the left, YL= young leaves) or roots (on the right) of *35S-UVR8* plants compared to the control. Values are averages ± SD (n = 3). **(B)** IAA conjugates in *uvr8-6* mutant plants. IAA was extracted from young leaves (1-6) and old leaves (7-10) of 21-day-old plants grown *in vitro* in a growth chamber at 23° C under a 16-h light/8h dark photoperiod or from roots of 7-day-old seedlings grown under continuous light. Values are averages ± SD (n = 3; *, P = 0.05).